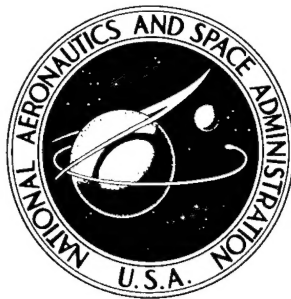


002488

f

NASA TECHNICAL NOTE



NASA TN D-3117

NASA TN D-3117

AMPTIAC

DISTRIBUTION STATEMENT A
Approved for Public Release
Distribution Unlimited

MONTE CARLO APPROACH
TO TOUCHDOWN DYNAMICS
FOR SOFT LUNAR LANDING

by Robert E. Lavender

*George C. Marshall Space Flight Center
Huntsville, Ala.*

20020319 122

NASA TN D-3117

MONTE CARLO APPROACH TO TOUCHDOWN
DYNAMICS FOR SOFT LUNAR LANDING

By Robert E. Lavender

George C. Marshall Space Flight Center
Huntsville, Ala.

NATIONAL AERONAUTICS AND SPACE ADMINISTRATION

For sale by the Clearinghouse for Federal Scientific and Technical Information
Springfield, Virginia 22151 - Price \$3.00

TABLE OF CONTENTS

	Page
SUMMARY	1
INTRODUCTION	1
VEHICLE CHARACTERISTICS	1
INITIAL CONDITIONS	4
TOUCHDOWN DYNAMICS PROGRAM	9
RESULTS	11
APPENDIX A. TOUCHDOWN CONDITIONS	37
APPENDIX B. RANDOM NUMBER GENERATOR CONFIDENCE TEST	47

LIST OF ILLUSTRATIONS

Figure	Title	Page
1.	Vehicle Configurations	17
2.	Spring Constants for Vehicles I, II, and III	18
3.	Force-Stroke Relationship	19
4.	Chi-square Frequency Function	20
5.	Chi-square Distribution Function	21
6.	Normal Distribution Function	22
7.	Surface and Body Axes Orientation	23
8.	Symmetric Heading Orientations	24
9.	Stability Boundary for Vehicle 3	25
10.	Stability Boundary for Vehicle 7	26
11.	Lower Limit Probability of Stable Landing	27

LIST OF TABLES

Table	Title	Page
1.	Geometric Properties of LFV, LEM, and LLS	28
2.	Geometric Properties of Vehicles I, II, and III	28
3.	Limiting Forces for Type I Vehicles	29
4.	Dynamic Scaling Factors	29
5.	Initial Conditions from Chi-Square Distribution	30
6.	Tabulation of Distribution Functions	31
7.	Summary of Touchdown Dynamics Runs for Vehicle 1	32
8.	Summary of Touchdown Dynamics Runs for Vehicle 5	34
9.	Summary of Cases which Tumble	35
10.	Sample Probability of Stable Landing	36
11.	Lower Limit Probability of Stable Landing	36

DEFINITION OF SYMBOLS

Symbol	Definition
C	Confidence coefficient
CSA	Velocity cross-slope angle (angle between total horizontal velocity vector and principal slope direction)
C_{mp}	Crushing force in main strut
C_{sp}	Crushing force in support strut
D	Landing gear diameter
g	Lunar gravity
k_v	Vertical spring constant per leg
k_z	Radius of gyration in pitch
L	Height of the center of gravity
m	Vehicle mass
n_f	Number of cases which tumble
n	Number of cases in sample
N	Number of legs
\bar{p}_s	Sample probability of stable landing
p_s	Lower confidence limit on probability of stable landing for binomial population
r	Radius from vehicle's centerline to main strut attachment point
\bar{V}_{ht}	Nondimensional total horizontal velocity
\bar{V}_v	Nondimensional vertical velocity
V_{ht}	Total horizontal velocity

DEFINITION OF SYMBOLS (Concluded)

Symbol	Definition
V_h	Component of horizontal velocity in the direction of principal slope
V_v	Vertical velocity
V_z	Component of horizontal velocity perpendicular to direction of principal slope
Y_a	Distance from bottom of vehicle to main strut attachment point
Y_p	Distance from landing gear foot pads to bottom of vehicle
α, β, γ	Dynamic scaling factors shown in Table 4
γ	Lunar Slope
θ_p	Vehicle's pitch angle referenced to the horizontal
θ_0	Initial pitch angle with respect to lunar surface
ϕ_0	Vehicle's initial heading orientation with respect to principal slope direction
ϕ_{03}	Equivalent heading orientation for three-legged vehicle
ϕ_{04}	Equivalent heading orientation for four-legged vehicle
σ	Standard deviation for normal distribution
ν	Degrees of freedom for chi-square distribution
ω	Angular velocity
ψ_0	Initial bank angle

MONTE CARLO APPROACH TO TOUCHDOWN DYNAMICS FOR SOFT LUNAR LANDING

SUMMARY

Results of analytical touchdown dynamics investigations are presented which were conducted to obtain estimates of the probability of stable landing for configurations with various landing gear diameters. Both three-legged and four-legged vehicles are considered in the analysis. Dynamic scaling considerations are taken into account so that the results are applicable to a wide range of vehicle size and mass. A Monte Carlo approach is taken in the determination of initial landing conditions. *[Spacecraft]*

Results indicate that for a given probability of stable landing, a three-legged vehicle requires a landing gear diameter only slightly larger than the diameter required for a four-legged vehicle. Therefore the three-legged vehicle's landing gear should weigh less. *[ind]*

INTRODUCTION

In the overall design and performance of spacecraft intended to soft-land on the moon, analysis of touchdown dynamics motion is an important part. Such analysis in the past has been restricted to specific missions and vehicles designed for those missions such as Surveyor (ref. 1), Lunar Excursion Module (ref. 2), Lunar Flying Vehicle (ref. 3), and Lunar Logistics System (ref. 4). In general, the analysis for each vehicle has not been a complete parametric study over a wide range of initial conditions, but rather a limited study with emphasis on what the vehicle can do under the worst set of conditions. The parametric approach is not feasible because of the large number of parameters involved. For example, if a parametric study of a particular vehicle is considered with only three variations of ten initial touchdown conditions, a total of three to the tenth power, or 59,049 combinations, is produced.

Presented in this report are results of a general touchdown dynamics study in which a Monte Carlo approach is taken to the determination of initial conditions. This approach is more realistic than simply choosing the worst-case conditions and does not require the prohibitive amount of analysis which a

parametric approach would require. The vehicle configurations used are determined in a standardized form, and the results are equally applicable to the Lunar Flying Vehicle, Lunar Excursion Module, or Lunar Logistics System, even though these vehicles vary greatly in size and mass.

Initial conditions have been determined using a Monte Carlo approach for 400 cases. For each case, the initial conditions were determined for 10 parameters: vertical velocity, horizontal velocity, velocity cross-slope angle, vehicle pitch, bank, and heading angles, lunar slope, and the vehicle's pitch, roll, and yaw rates at touchdown. The coefficient of friction between the landing pads and lunar surface is assumed to be infinite (no sliding). Eight generalized vehicles are analyzed for these 400 cases to determine whether or not the vehicle being considered lands safely or tumbles. The eight vehicles considered correspond to three-legged and four-legged vehicles with four variations in the ratio of landing gear diameter to center-of-gravity height. From these results, an estimate is made of the probability of stable landing on the lunar maria for each of the eight vehicles.

The author is indebted to Mr. John D. Capps, Computation Laboratory, who programmed the equations for the three-dimensional touchdown dynamics digital program as well as the program used in the determination of initial conditions.

VEHICLE CHARACTERISTICS

The Lunar Flying Vehicle (LFV) is a small vehicle which has received consideration for lunar surface exploration after the initial Apollo landings. Primary emphasis has been placed upon a vehicle having an 80-kilometer maximum range when carrying a payload of two men with their portable life support systems. The primary mission for such a vehicle was considered to be rescue back to the Lunar Excursion Module (LEM) from a disabled surface roving vehicle. A secondary mission was that of supplementing the roving vehicle by permitting flights into areas which are inaccessible to a roving vehicle.

The Lunar Logistics System (LLS) is a large cargo-carrying vehicle which has received study as a means of delivering 15-ton payloads to the moon in support of a lunar base.

Even though the three spacecraft (LFV, LEM, LLS) vary greatly in size and mass, all three vehicles can be reduced to approximately the same nondimensional geometry as shown in Table 1. As a result of this, three standard vehicles (I, II, and III) have been established which are representative of the LFV, LEM,

and LLS size vehicles. The standardized dimensions are shown in Table 2. The radius of gyration about the bank (roll) axis is assumed equal to that shown for pitch. The radius of gyration in yaw (about the vehicle's centerline) is taken to be 0.9 times the pitch value. Having standardized the three vehicles, all touch-down dynamics calculations performed for Vehicle I can be made applicable through dynamic scaling factors to Vehicle II and Vehicle III.

Eight vehicles are considered, as shown in Figure 1, corresponding to four values of the ratio of landing gear diameter to center-of-gravity height. Both three-legged and four-legged vehicles are considered even though the LFV, LEM, and LLS have all received major emphasis as four-legged vehicles. A major purpose of this study, however, is to obtain estimates of the relative probability of stable landing with three-legged vehicles compared to four-legged vehicles. Although the diameter--c.g. height ratios for LFV, LEM, and LLS vary from 2.50 to 3.25 (Table 1), the values chosen for this generalized study vary from 2.0 to 3.0. The large landing gear diameter designed for the LLS was based upon very severe initial conditions which are believed to be overly conservative, resulting in an excessively heavy landing gear.

The spring rates assumed for the vehicles of this study (Fig. 2) are the equivalent vertical spring rates per leg when landing on a level, high-friction surface with no sliding of the foot pads. These vertical spring rates were obtained by assuming an elastic spring rate (7005 N/cm or 4000 lb/in for Vehicle I) along the three struts of an inverted tripodal leg. As seen, the vertical spring rate decreases as the landing gear diameter increases, negating somewhat the beneficial result of the larger landing gear diameters. The spring rates assumed for the LLS size vehicle (Type III) are rather large and may be very difficult to obtain. These spring rates are required to satisfy dynamic similarity. The results of this study may therefore be somewhat optimistic for this larger vehicle because of the high stiffness assumed. On the other hand, the assumed spring rate for Vehicle I (LFV) is probably low so that the results obtained may be somewhat pessimistic. Previous study (ref. 5) has shown that decreasing stiffness has a detrimental effect on landing stability.

The force-stroke relationship in each strut is shown in Figure 3. Upon compression, each strut is assumed to compress elastically until the limiting force in compression is reached. Further stroking takes place with a constant stroking force assumed. As the strut begins to re-extend, the stored elastic energy is released until the strut force reaches zero. Further re-extension of the strut takes place under zero load or free-return conditions. No limiting force in tension is assumed. The same spring constant is assumed for the strut in tension as used in compression. The limiting force is assumed to represent the crushing force of aluminum honeycomb energy absorbers in the struts. Upon subsequent stroking, the strut shortens under zero load as long as it is still in the free-return stroking region.

The limiting force or crushing force values for the eight vehicles were determined so that the deceleration load factor is limited to 3.0 earth g's when the vehicle lands on a level, high friction surface on all legs simultaneously. This load factor appears to be a good choice from previous study (ref. 6). If the chosen load factor is too high, a landing gear designed for such loads is too heavy. If the load factor is too low, excessive stroking is required to absorb the landing energy, thus increasing the strut length required and landing gear weight. Each leg is considered to be an inverted tripodal arrangement of one main strut and two lower support struts. The limiting force of each support strut is considered to be one-third of the main strut limiting force. This relationship is believed to be a good choice based upon previous analysis (ref. 7). The limiting forces obtained for the eight vehicles are shown in Table 3. These values correspond to the forces for Vehicle I (LFV). Corresponding forces for the larger vehicles are increased by the dynamic similarity force factors given in Table 4.

The mass of Vehicle I (LFV) is considered to be 453.59 kg (earth weight of 4448 N or 1000 lb). The mass ratios given in Table 4 can be used to obtain the mass of the larger vehicles.

INITIAL CONDITIONS

Initial conditions have been obtained using a Monte Carlo approach which randomly selects values from zero to one and relates these values to the initial conditions sought through the distribution functions that have been established for the initial variables. Determining a reasonable distribution function for each of the variables of interest is the most questionable part of the entire study because of the lack of data. However, one value of this study may be that of helping to point out the need for detailed and realistic statistical information concerning initial touchdown conditions.

Various simulations have been performed (refs. 8-13) which have yielded some information on the conditions at touchdown for lunar landing. All of these simulations have been conducted with varying degrees of realism relative to instrumentation and control response, pilot training, test objectives, pilot motivation, and other factors. Results must be viewed with some degree of caution since they may not realistically simulate an actual vehicle with well trained and motivated pilots. Future efforts, it is hoped, will provide more realistic information on touchdown conditions through the use of the Lunar Landing Research Facility (ref. 14) and also the free flight Lunar Landing Vehicle (ref. 15).

As far as the vertical and horizontal components of touchdown velocity are concerned, it is reasonable to expect that the vast majority of cases of actual landings with well motivated pilots will be very soft landings with low touchdown

velocities. The simulations reported by Hill (ref. 9) show that the vertical descent rate is less than 1.2 m/s (4 fps) for 90 percent of the cases. The forward velocity at touchdown was also reported as less than 0.6 m/s (2 fps) for 90 percent of the cases. The simulation results reported by Wood and Post (ref. 12) indicate more severe landing velocities. About 35 percent of the time the pilots failed to land within the design envelope of 3.0 m/s (10 fps) vertical velocity, and 1.5 m/s (5 fps) horizontal velocity. It was concluded that this large failure rate can be attributed not only to difficulty of the task, but also to the training level of the pilots and limitations in the simulation. It was believed that greater pilot experience, and improvements in displays and display precision will reduce such failures considerably in future studies.

It is expected that the frequency functions of the vertical and horizontal velocity components should have some tail-off toward higher velocities to represent more severe cases. The frequency function chosen as a reasonable representation of the vertical and horizontal velocity components is given in Figure 4. This function corresponds to the chi-square frequency function with three degrees of freedom. Appropriate choices for multiplication constants convert the values of the variable x to the vertical and horizontal velocities.

Concerning the lunar slope expected in maria regions of the moon, it is expected that the vast majority of landings will be on low sloped terrain with only a small percent of the landings on rougher terrain. It may well be argued that manned landings on rough, highly sloped terrain will never take place. However, for the small LFV exploration system, some landings may well be on steeper slopes because of the desire to land near interesting geological and topological features. In addition, if lunar dust somewhat clouds the pilot's vision during the final phase of landing, it is possible that one or more pads may impact on a protuberance or into a depression which would increase the effective landing slope. In addition, the pad-surface interaction during impact may well serve to increase the effective landing slope. Experimental evidence (refs. 16-17) indicates that the bearing strength of the soil is not the sole criterion for penetration. There is a tendency for the downhill pads to penetrate the soil more deeply than the uphill pads during a landing, and thus increase the effective landing slope. Considering these factors, it is assumed that the frequency function shown in Figure 4 is also a reasonable approximation of the effective slope to be encountered upon landing. Mason and colleagues (ref. 18) have established a similar highly skewed frequency function for a representative lunar surface profile from 20 100-kilometer traverses. Their work was performed to establish a baseline for determining lunar roving vehicle requirements. An appropriate choice of a multiplication factor converts the variable x in Figure 4 into the effective lunar slope.

The distribution (cumulative frequency) function, shown in Figure 5, is used in the Monte Carlo approach to obtain vertical and horizontal velocity components and the effective lunar slope. The values given in Table 5 have been obtained

from this distribution function by use of appropriate multiplication constants. The multiplication constants were chosen on the basis of the values emphasized in Table 5. For example, McCauley indicates (ref. 19) that, in the 1-10 meter scale, the median slope of the maria is about 5 degrees. Thus, with the assumed distribution, 20 percent of the maria has a slope of about 2 degrees or less, 80 percent is within 10 degrees, and 1 percent is 24 degrees or more.

For the LEM size (Type II) vehicle, it is assumed that 99.865 percent of the landings will have a vertical velocity of 3.048 m/s (10 fps) or less, and a horizontal velocity of 1.524 m/s (5 fps) or less. Thus, with the assumed distribution, 90 percent of the landings have a vertical velocity of 1.188 m/s (3.90 fps) or less, and a horizontal velocity of 0.594 m/s (1.95 fps) or less. While the values were based upon the LEM design values of 10 fps and 5 fps (ref. 12), the 90 percentile values also correspond quite well with the simulation results of Hill (ref. 9). Thus, it is considered that the LEM size vehicle (Type II) will land 50 percent of the time with a vertical velocity of 0.448 m/s (1.47 fps) or less, with a horizontal velocity of 0.224 m/s (0.735 fps) or less.

For the results to be equally applicable to the LFV size (Type I) vehicle and the LLS size (Type III) vehicle, the velocities (also shown in Table 5) were adjusted by dynamic scaling considerations. For example, it is assumed that 90 percent of the landings for the LLS (Type III) vehicle will be with a vertical velocity of 1.638 m/s (5.374 fps) or less. For the LFV (Type I) vehicle, it is assumed that 90 percent of the landings will occur with a vertical velocity of 0.706 m/s (2.32 fps) or less.

The dynamic scaling factors given in Table 4 show that, for dynamic similarity, the velocity is scaled as the square root of the vehicle's linear dimension when landing in the same gravity field. Thus, for larger vehicles, larger landing velocities can be tolerated. While this indicates that the larger vehicles may be easier to land, this table also shows that the spring rate for dynamic similarity is proportional to the mass and inversely proportional to the linear dimension when landing in the same gravity field. Thus, since the mass increases to some power of the linear dimension, higher spring rates are required for the larger vehicles for dynamic similarity.

The horizontal velocity is assumed to be controlled as far as possible to be zero. Therefore, it is considered that the direction of the horizontal velocity vector at touchdown with respect to the principal slope direction has an equal probability of being in any direction. Further study of this problem may show an advantage to having a horizontal velocity of sufficient magnitude to guarantee an uphill landing rather than a smaller residual component that may be in the downhill direction. The assumption of trying to land at zero horizontal velocity, however, should certainly be applicable to unmanned vehicles such as the LLS or an unmanned LEM used as a LEM truck. It is also assumed that the vehicle's

geometric heading orientation with respect to the principal slope direction has an equal probability of being in any direction. This assumption is applicable to unmanned vehicles and also to manned vehicles where vision impairment due to lunar dust might make the determination of the direction of principal slope difficult. Under clear vision, the pilot would probably orientate the vehicle's heading to align in a 1-2-1 orientation to the slope for improved stability.

The pitch and bank angles at touchdown, referenced to the horizontal, are assumed to follow a normal distribution with zero mean. Likewise, the vehicle's angular rates in pitch, roll, and yaw are also assumed to follow the same distribution. The normal distribution with zero mean and standard deviation of one is shown in Figure 6. Appropriate multiplication constants convert the x variable to angles and angular rates. The standard deviation for pitch and bank angles is considered to be 2 degrees and is applicable for Vehicles I, II, and III. The standard deviation of pitch, roll, and yaw rates is taken to be 1.60 degrees per second for the Type II (LEM size) vehicle. Past simulation studies show that these are reasonable assumptions. For dynamic similarity, the corresponding standard deviation of angular rate is taken to be 2.70 degrees per second for the Type I (LFV) vehicle and 1.16 degrees per second for the Type III (LLS) vehicle.

The 10 variables of vertical velocity, horizontal velocity, lunar slope, cross-slope angle, heading angle, bank angle, pitch angle, pitch rate, roll rate, and yaw rate are assumed to be uncorrelated.

The Monte Carlo procedure for obtaining the initial conditions can be summarized in the following manner. A set of values for 400 cases is obtained where each case consists of obtaining 10 pseudo-random numbers from a previously developed digital random number generator subroutine for a rectangular frequency function (ref. 20). These numbers are equal to or greater than zero and equal to or less than one. These 10 random numbers, RN_1 through RN_{10} , are then used as $F(x_1)$ through $F(x_{10})$ to obtain the values for x_1 through x_{10} from Table 6.

This table was obtained from values tabulated by Abramowitz and Stegun (ref. 21). Linear interpolation is used to obtain the values of x_1 to x_{10} . The initial conditions are then computed:

$$\bar{V}_{ht} = 0.0605 x_1 \quad (1)$$

$$V_{ht} = \sqrt{g k_z} \bar{V}_{ht} \quad (2)$$

$$\bar{V}_v = 0.121 x_2 \quad (3)$$

$$V_v = \sqrt{g k_z} \bar{V}_v \quad (4)$$

$$\gamma = 2.113 x_3 \quad (5)$$

$$CSA = 360 x_4 \quad (6)$$

$$V_h = V_{ht} \cos CSA \quad (7)$$

$$V_z = - V_{ht} \sin CSA \quad (8)$$

$$\phi_0 = 360 x_5 \quad (9)$$

$$\psi_0 = 2 x_6 \quad (10)$$

$$\theta_p = 2 x_7 \quad (11)$$

$$\theta_0 = \theta_p + \gamma \quad (12)$$

$$\omega_x = 2.7 x_8 \quad (13)$$

$$\omega_y = 2.7 x_9 \quad (14)$$

$$\omega_z = 2.7 x_{10} \quad (15)$$

The values were obtained corresponding to the Type I (LFV) vehicle for convenience in performing touchdown dynamics computations since the time required to obtain the touchdown motion is less. A computing interval of 0.002 sec was used in performing the touchdown dynamics computations. The same results could have been obtained with the larger vehicles in the same computation time by increasing the computing interval by the appropriate time factors given in Table 4. Tabulation of the initial conditions for the 400 cases is given in Appendix A.

A random number confidence test was performed to judge the adequacy of the pseudo-random numbers generated by the digital subroutine. The results are given in Appendix B. Four thousand random numbers were generated corresponding to 400 cases with 10 random numbers in each case, RN_1 through RN_{10} , used to obtain the 10 initial conditions. Therefore, 400 values were obtained for each of the 10 random numbers RN_1 through RN_{10} . The range from zero to one was divided into 10 intervals so that these 400 values would have an expected frequency of 40 in each interval. The observed frequencies were obtained and the chi-square value obtained. These chi-square values should follow a chi-square distribution with 9 degrees of freedom. Therefore, the value of chi-square could be expected to exceed 12.2 (ref. 21) for 20 percent of the cases, or for 2 of the 10 random numbers. None of the random numbers have a chi-square value which exceeds the 12.2 value. Therefore, the values generated by the random number subroutine are adequate.

TOUCHDOWN DYNAMICS PROGRAM

The touchdown dynamics program used for this study corresponds to a three-dimensional method programmed for digital computer operations. The method was developed as a simplified version of the landing dynamics method of analysis for the LEM described by Mantus, Lerner, and Elkins (ref. 22). This simplified version is restricted to landings on a plane sloping surface without protuberances or depressions and without sliding of the landing pads along the surface. The surface and body axes orientation used is shown in Figure 7. The velocity cross-slope angle is the angle from the principal slope direction to the total horizontal velocity vector. The vehicle's heading angle defines the orientation of the vehicle's landing pads. Zero heading angle corresponds to a 1-2-1 pad orientation for a four-legged vehicle and to a 1-2 pad orientation for a three-legged vehicle. Heading angles of ± 45 degrees correspond to a 2-2 pad orientation for the four-legged vehicle. Heading angles of ± 60 degrees correspond to a 2-1 pad orientation for the three-legged vehicle. These various orientations are shown in Figure 8.

As previously stated, the initial heading orientation has been taken to have equal probability of being in any direction (360 degrees). However, as far as the touchdown dynamics program is concerned, 0, 90, 180, 270, and 360 degrees heading orientation is still a 1-2-1 orientation for a four-legged vehicle. Similarly, 0, 120, 240, and 360 degrees heading orientation is still a 1-2 orientation for a three-legged vehicle. Consequently, the initial heading angle obtained from the Monte Carlo analysis has been converted to an equivalent heading within ± 45 degrees for the four-legged vehicle and within ± 60 degrees for the three-legged vehicle for input into the touchdown dynamics program. Thus:

$$\phi_{04} = \phi_0 \quad , \quad 0 \leq \phi_0 \leq 45 \quad (16)$$

$$\phi_{04} = \phi_0 - 90 \quad , \quad 45 < \phi_0 \leq 135 \quad (17)$$

$$\phi_{04} = \phi_0 - 180, \quad 135 < \phi_0 \leq 225 \quad (18)$$

$$\phi_{04} = \phi_0 - 270, \quad 225 < \phi_0 \leq 315 \quad (19)$$

$$\phi_{04} = \phi_0 - 360, \quad 315 < \phi_0 \leq 360 \quad (20)$$

and

$$\phi_{03} = \phi_0 \quad , \quad 0 \leq \phi_0 \leq 60 \quad (21)$$

$$\phi_{03} = \phi_0 - 120, \quad 60 < \phi_0 \leq 180 \quad (22)$$

$$\phi_{03} = \phi_0 - 240, \quad 180 < \phi_0 \leq 300 \quad (23)$$

$$\phi_{03} = \phi_0 - 360, \quad 300 < \phi_0 \leq 360 \quad (24)$$

These equivalent heading angles for the 400 cases are also tabulated in Appendix A.

Each run begins with the vehicle's lowest pad just touching the surface. Strokes and forces along the struts are computed with subsequent determination of forces and moments referred to the body axes. The moments are used to obtain the angular accelerations about the body axes and are integrated numerically to obtain the angular velocities about the body axes. The rate of change of the angles θ , ψ , and ϕ are then computed from expressions containing the angular velocities about the body axes. The angular accelerations of $\ddot{\theta}$, $\ddot{\psi}$, $\ddot{\phi}$ are then obtained by equations derived from differentiating the equations for $\dot{\theta}$, $\dot{\psi}$, $\dot{\phi}$. The angles θ , ψ , and ϕ are obtained by numerical integration using the computed rates and angular accelerations for these angles. The forces computed are converted to forces along the inertial (surface) axes and the vehicle's translational accelerations obtained. These accelerations are integrated numerically to obtain the velocity and position of the vehicle's center of gravity. The computations are repeated at each time step until sufficient time has elapsed to determine whether or not the vehicle tumbles or is stable.

As long as a pad is off the surface, it travels along with the vehicle. Upon reaching the surface, the pad remains at its impact position until the forces on the pad normal to the surface become negative. The negative force is set to zero and the pad then lifts from the surface and again travels along with the vehicle until it impacts the surface again.

Examples of stability boundaries which have been obtained by this program are shown in Figures 9 and 10. Figure 9 gives the stability boundary in terms of the lunar slope versus the vehicle's heading angle for a three-legged vehicle. Figure 10 gives corresponding results for a four-legged vehicle. As seen from Figure 9, stable landings can be made on lunar slopes from 6 degrees to 18 degrees depending upon the vehicle's heading orientation with respect to the principal slope direction. For the four-legged vehicle (Fig. 10), stable landings can be made on slopes from 10 degrees to about 18 degrees. Minimum stability does not correspond to 45 degrees heading (2-2 orientation) but rather to a heading angle of about 30 degrees for this case. The impact velocity values shown correspond to the small (Type I) vehicle.

RESULTS

With the three-legged vehicle having the smallest landing gear (Vehicle 1), the 400 cases were reviewed to determine by inspection which cases were more likely to tumble. Most of the cases are obviously stable because of the small touchdown velocities, combined with small surface slopes. Three of the cases were considered to obviously tumble because of the surface slope being greater than 24 degrees. Touchdown dynamics motion was then computed for 45 cases which were believed to have a substantial probability of tumbling. Of these, 14 cases did result in tumbling motion.

Based upon these results, touchdown motion was computed for an additional 34 cases which were believed to be stable, but with a substantial degree of uncertainty. Of these, three cases tumbled. Finally, an additional nine cases were chosen which were thought definitely would be stable but lacked the high degree of certainty desired. Of these, none tumbled. Based upon these results, a final review was made of the remaining cases with the conclusion that all would certainly be stable. Therefore, for Vehicle 1, 20 cases of the 400 correspond to tumbling cases.

A summary of the cases used for the touchdown dynamics computations for Vehicle 1 is given in Table 7. It is observed that tumbling resulted for Case 43 with a lunar slope of only 6.9 degrees while Case 332, with a lunar slope of 19.2 degrees, was stable. While the lunar slope is a very important parameter to consider in touchdown dynamics analysis, other initial conditions are also obviously important. Case 43 corresponds to a near 1-2 landing orientation with a relatively high vertical impact velocity, while Case 332 corresponds to a near 2-1 orientation with a small impact velocity.

Touchdown dynamics motion was then computed using Vehicle 2 for the 20 cases which were previously determined as tumbling cases. All stable cases for Vehicle 1 would also be stable cases for Vehicle 2 since nothing is changed except the landing gear diameter, which is larger. Of these 20 cases, 11 cases tumbled including the 3 cases considered obvious for Vehicle 1.

Touchdown motion was then computed using Vehicle 3 for the 11 cases which tumbled when using Vehicle 2. Of these, four cases tumbled.

Touchdown motion was then computed using Vehicle 4 for the four cases which tumbled when using Vehicle 3. Of these, none tumbled.

A similar analysis was performed for the four-legged vehicles. Vehicle 5 was used and touchdown dynamics was computed for 25 cases which were thought to have a substantial probability of tumbling. Of these, 11 cases tumbled.

Computations were then performed for 32 additional cases which were believed to be stable, but with a substantial degree of uncertainty. Of these, three cases tumbled. Finally, an additional 14 cases were considered which were thought definitely would be stable but lacked the high degree of certainty desired. Of these, none tumbled. Three cases (with a slope of over 24 degrees) were considered to be obviously tumbling cases. Therefore, for Vehicle 5, 17 of the 400 cases correspond to tumbling cases.

A summary of the cases used for touchdown dynamics calculations for Vehicle 5 is given in Table 8. No case tumbled corresponding to a lunar slope of less than 15.5 degrees, while no case was stable with a slope greater than 19.3 degrees. This is a slope spread of only 3.8 degrees compared to a slope spread of 12.3 degrees for the corresponding three-legged vehicle (Vehicle 1). While 7 cases tumbled for Vehicle 1 with a lunar slope of less than 15.5 degrees, only 13 cases tumbled with lunar slopes of 15.5 degrees or more compared to the 17 cases for Vehicle 5. These results indicate that a relatively well defined critical slope can be established for four-legged vehicles compared to three-legged vehicles.

The vehicle with the next largest diameter (Vehicle 6) was then considered. Touchdown motion was computed for the 17 cases with the result that 7 cases tumbled including the 3 cases considered obvious for Vehicle 5. These seven cases were then considered using Vehicle 7 with the result that three cases tumbled. Finally, these three cases were considered using Vehicle 8 with the result that none tumbled. The cases corresponding to tumbling motion are summarized in Table 9.

A summary of the sample probabilities for stable landing is given in Table 10. The sample probability of stable landing varies from 0.950 for the three-legged vehicle with the smallest landing gear to 1.000 for the vehicles with the largest landing gear. The lower limit probability for stable landing with 0.95 and 0.995 confidence coefficients for the binomial population has been taken from published tables (ref. 23) based upon the sample size of 400. These results are given in Table 11. The table also shows the lower limit probability for stable landing based upon an approximate equation given by Dalton (ref. 24). This equation is

$$p_s = \left[\frac{(1-C)/e^{n_f}}{[(3+2C)/4]^{\delta/(n-n_f/2)}} \right] \quad (25)$$

where

$$\delta = 0 \quad \text{for } n_f = 0$$

$$\delta = 1 \quad \text{for } n_f \neq 0.$$

This equation is seen to give a very good approximation of the results for the binomial population.

The lower limit probability for stable landing for the binomial population with a confidence coefficient of 0.995 is shown in Figure 11. Since neither Vehicle 4 nor Vehicle 8 had any cases which tumbled, touchdown dynamics runs were also made for an additional three-legged vehicle and an additional four-legged vehicle with a diameter-c. g. height ratio of 2.75. The three-legged vehicle tumbled for Case 317. This case has the highest lunar slope (28.2 degrees) of the 400-case sample and the vehicle lands in a near 1-2 orientation. The resulting probability for stable landing for this vehicle is also shown in Figure 11. The four-legged vehicle tumbled for Case 129 and also for Case 317. Case 129 has the second highest lunar slope (27.3 degrees) of the 400-case sample. The resulting probability for stable landing is also shown in Figure 11.

The probability values for the three-legged vehicles vary in a smooth manner, whereas the values for the four-legged vehicles are somewhat erratic. At a diameter-c. g. height ratio of 2.75, the probability of stable landing for the four-legged vehicle is less than for the three-legged vehicle based upon the 400-case sample. It is believed that this result would not be obtained if the sample size were increased by an order of magnitude. Similarly, at a diameter-c. g. height ratio of 2.25, the probability of stable landing for the four-legged vehicle appears to be somewhat high. Consequently, the curve shown in Figure 11 for the four-legged vehicles has been faired in a manner to remove the erratic nature of the data points.

The results indicate that, for a given probability of stable landing, a three-legged vehicle requires a landing gear diameter only slightly larger than the diameter required for a four-legged vehicle. Since each leg is folded for flight to the moon and must be deployed before landing, the reliability of landing gear deployment should be greater for a three-legged vehicle. With only three landing pads to contact the surface, there is less chance of contacting a protuberance or depression. A three-legged vehicle assures a more positive final resting support, whereas a four-legged vehicle may tend to rock back and forth. With only a slightly larger diameter required, the three-legged vehicle's landing gear should weigh less.

George C. Marshall Space Flight Center,
National Aeronautics and Space Administration,
Huntsville, Alabama, September 30, 1965

REFERENCES

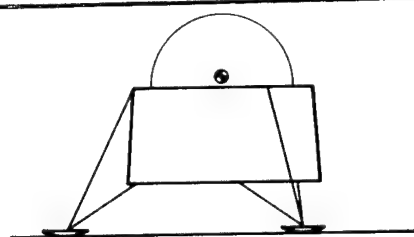
1. Deitrick, R. E. and Jones, R. H.; Surveyor Spacecraft System - Touchdown Dynamics Study, Report SSD-3030R, Hughes Aircraft Company, January 1963.
2. LEM Familiarization Manual; Report LMA 790-1, Grumman Aircraft Engineering Corp., July 15, 1964.
3. Final Report, A Study of Lunar Flying Vehicles; Report 7217-928001, Bell Aerosystems Company, June 1965.
4. Lunar Logistic System; Report MTP-M-63-1 Vol. I-XI, NASA Marshall Space Flight Center, March 15, 1963. (Confidential)
5. Aero-Astroynamics Research Review No. 1; NASA TM X-53189, October 1, 1964.
6. Lavender, Robert E.; Touchdown Dynamics Analysis of Spacecraft for Soft Lunar Landing, NASA TN D-2001, January 1964.
7. Black, Raymond J.; Quadrupedal Landing Gear Systems for Spacecraft, AIAA J. Spacecraft, Vol. 1. No. 2, 1964.
8. Markson, E., Bryant, J., and Bergsten, F.; Simulation of Manned Lunar Landing, Lunar Missions Meeting, American Rocket Society, July 1962, (ARS Preprint 2482-62).
9. Hill, J. A.; A Piloted Flight Simulation Study to Define the Handling Qualities Requirements for a Lunar Landing Vehicle, Report NA62H-660, North American Aviation, September 13, 1962.
10. Rolls, Stewart L., and Drinkwater, III, Fred J.; A Flight Evaluation of Lunar Landing Trajectories Using a Jet VTOL Test Vehicle, NASA TN D-1649, February 1963.
11. Matranga, Gene J., Washington, Harold P., Chenoweth, Paul L., and Young, William R.; Handling Qualities and Trajectory Requirements for Terminal Lunar Landing as Determined from Analog Simulation, NASA TN D-1921, August 1963.
12. Wood, F. E., and Post, S.; Final Report, Lunar Landing Simulation IIIA, Report LED-570-4, Grumman Aircraft Engineering Corp., April 1, 1964.

REFERENCES (Continued)

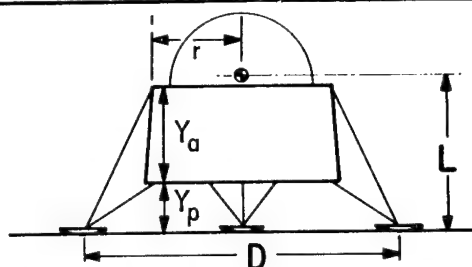
13. Hatch, Howard G., Jr., Algranti, Joseph S., Mallick, Donald L., and Ream, Harold E.; Crew Performance During Real-Time Lunar Mission Simulation, NASA TN D-2447, September 1964.
14. Jaquet, Byron M.; Simulator Studies of Space and Lunar Landing Techniques, Fifth Annual Lectures in Aerospace Medicine, USAF School of Aerospace Medicine, February 3-7, 1964.
15. Feasibility Study for a Lunar Landing Flight Research Vehicle, Report No. 7161-950001, Bell Aerosystems Company, March 8, 1962.
16. Final Report of Lunar Landing Dynamics Systems Investigation, Report MM-64-8, Bendix Products Aerospace Division, October 1964.
17. Final Report; Lunar Landing Dynamics Specific Systems Engineering Studies, Report MM-65-4, Bendix Products Aerospace Division, June 1965.
18. Mason, R. L., McCombs, W. M., and Cramblit, D. C.; Engineering Lunar Model Surface (ELMS), Report TR-83-D, Kennedy Space Center, September 4, 1964.
19. McCauley, John F.; A Preliminary Report on the Terrain Analysis of the Lunar Equatorial Belt, Report Unnumbered, Geological Survey, U. S. Department of Interior, July 1, 1964.
20. Lester, Roy C.; Probability of S-IVB/IU Lunar Impact Due to Guidance Errors at Translunar Injection, NASA TM X-53134, September 21, 1964. (Confidential)
21. Abramowitz, M., and Stegun, I. A. (editors); Handbook of Mathematical Functions, Applied Mathematics Series (AMS) 55, National Bureau of Standards, June 1964.
22. Mantus, M., Lerner, E., and Elkins, W.; Landing Dynamics of the Lunar Excursion Module - Method of Analysis, Report LED-520-6, Grumman Aircraft Engineering Corporation, March 6, 1964.
23. Lipow, M.; Tables of Binomial Upper Confidence Limits on Probability of Failure, Report 6120-0008-MU-000, Space Technology Laboratories, July 1962.

REFERENCES (Concluded)

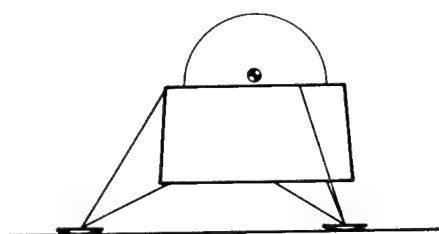
24. Dalton, Charles C.; Estimation of Tolerance Limits for Meteoroid Hazard to Space Vehicles 100-500 Kilometers Above the Surface of the Earth, NASA TN D-1996, February 1964.



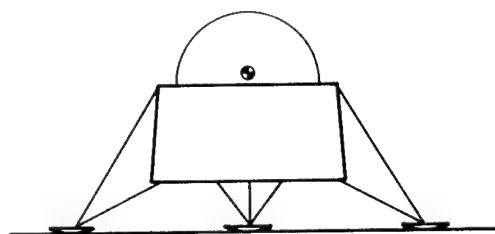
Vehicle 1, $N=3$, $D/L=2.0$



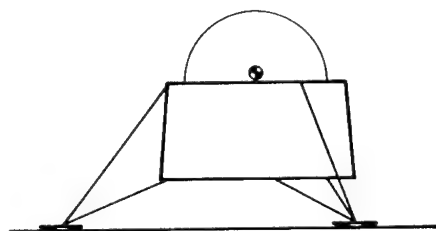
Vehicle 5, $N=4$, $D/L=2.0$



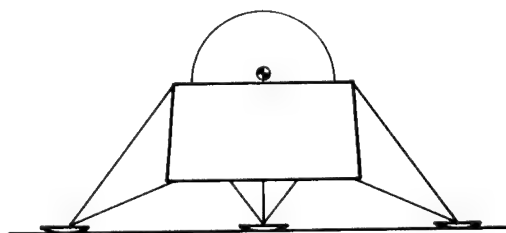
Vehicle 2, $N=3$, $D/L=2.25$



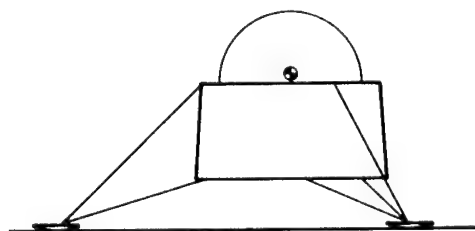
Vehicle 6, $N=4$, $D/L=2.25$



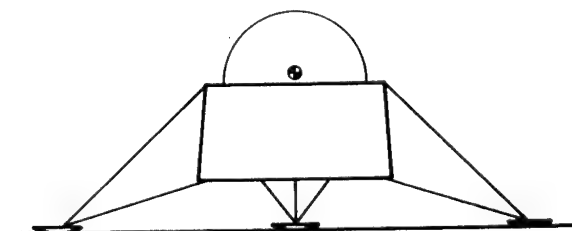
Vehicle 3, $N=3$, $D/L=2.5$



Vehicle 7, $N=4$, $D/L=2.5$



Vehicle 4, $N=3$, $D/L=3.0$



Vehicle 8, $N=4$, $D/L=3.0$

FIGURE 1. VEHICLE CONFIGURATIONS

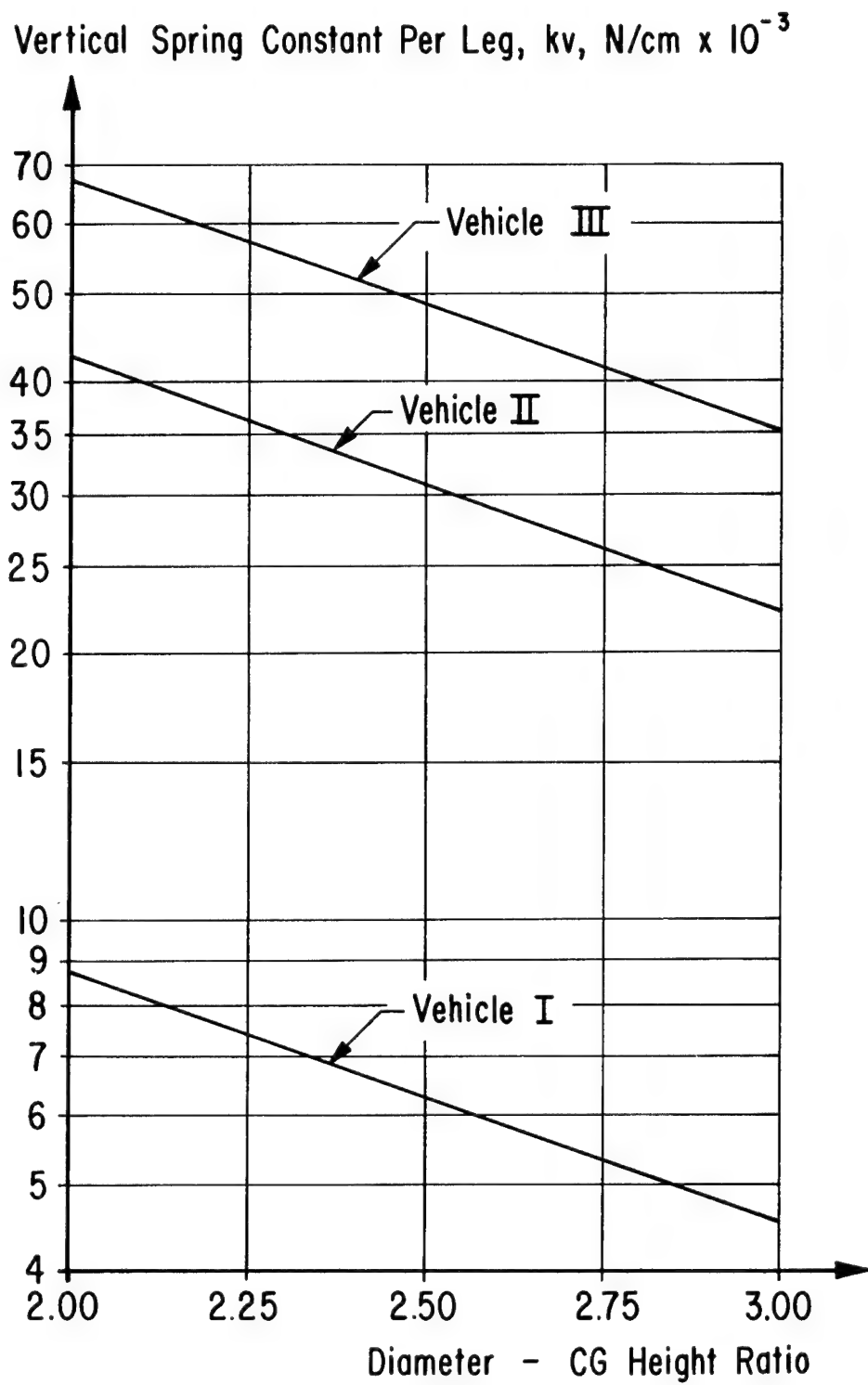


FIGURE 2. SPRING CONSTANTS FOR VEHICLES I, II, AND III

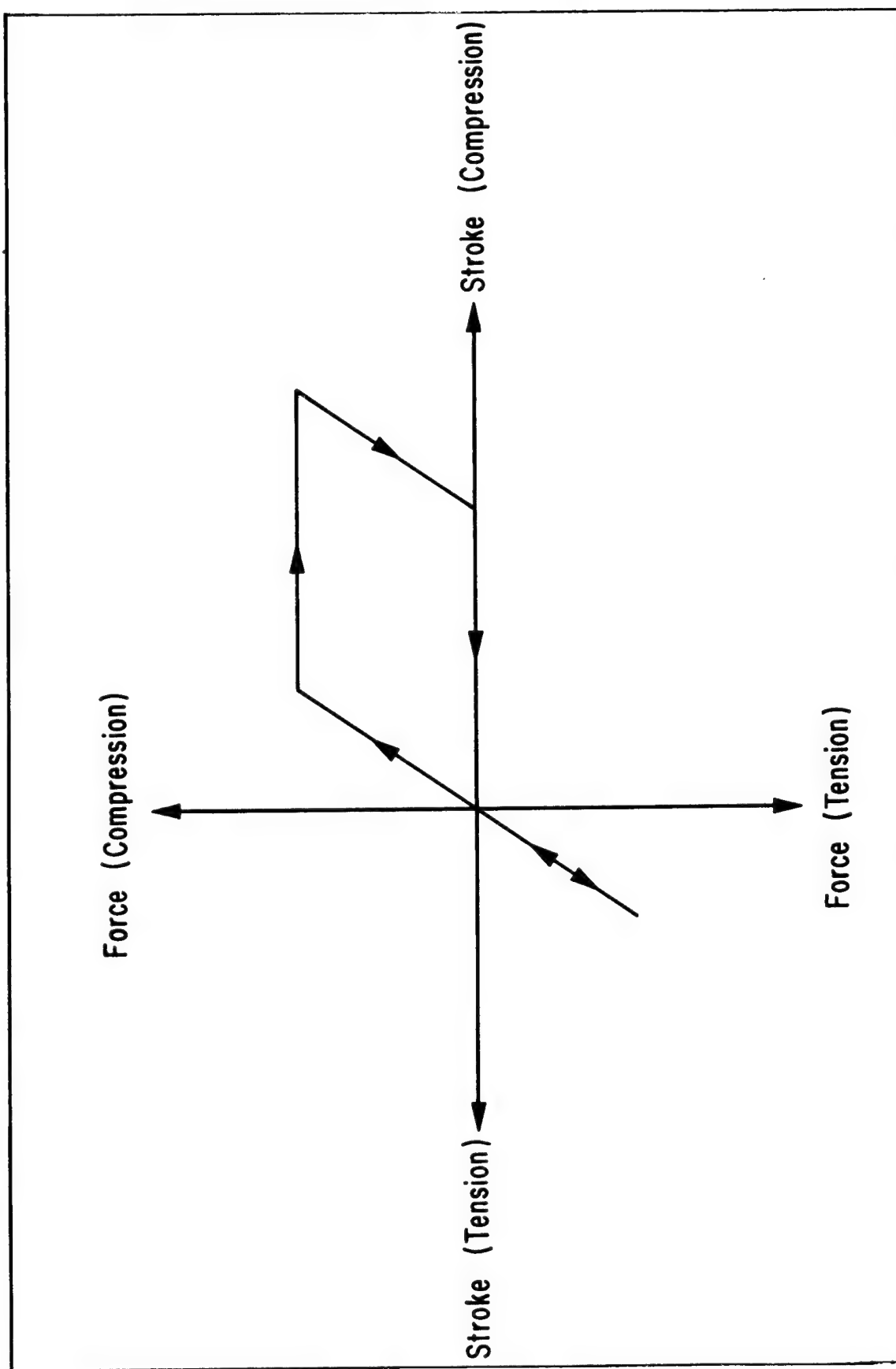


FIGURE 3. FORCE-STROKE RELATIONSHIP

$$f(x) = \frac{(x)^{\frac{v}{2}-1} e^{-x/2}}{2^{v/2} \Gamma(\frac{v}{2})}; v=3$$

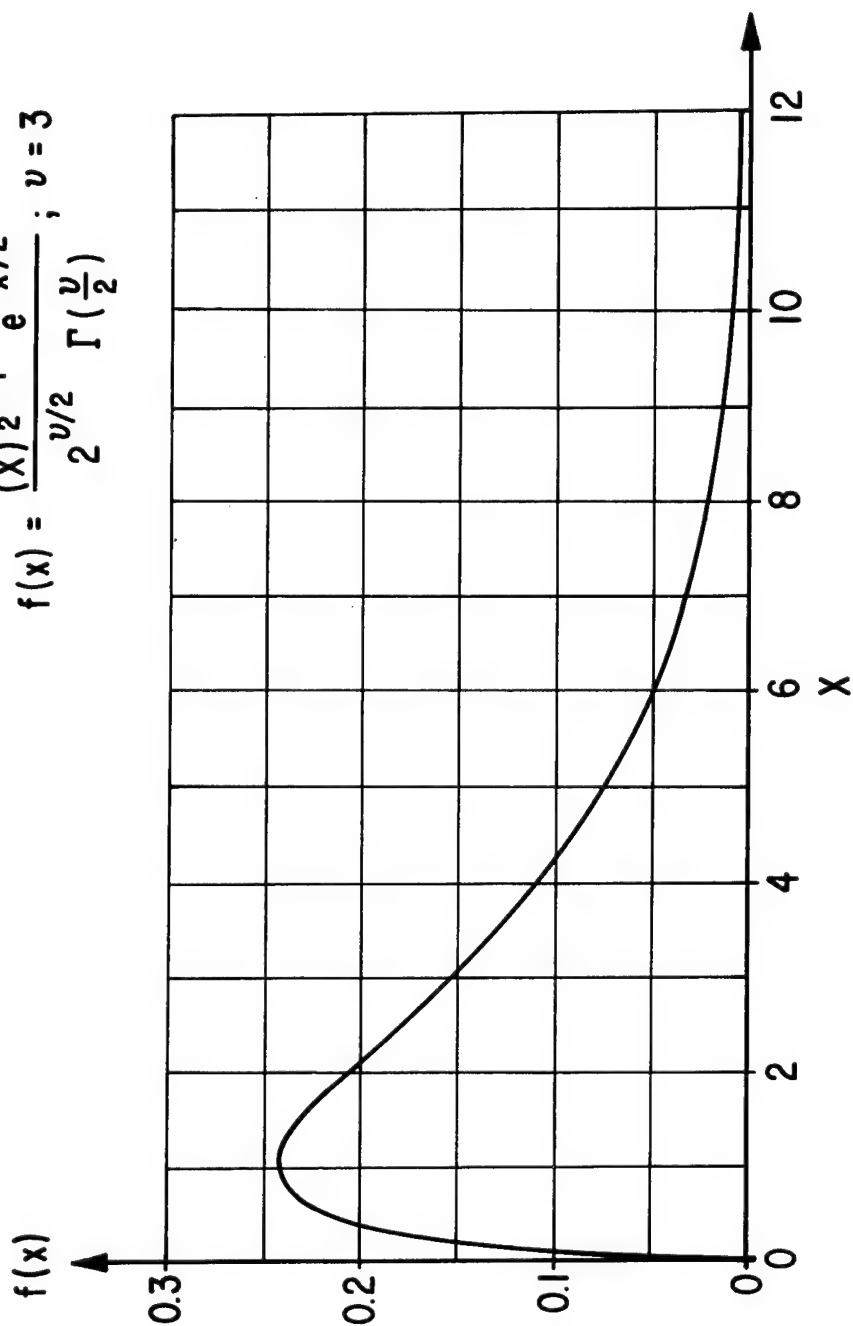


FIGURE 4. CHI-SQUARE FREQUENCY FUNCTION

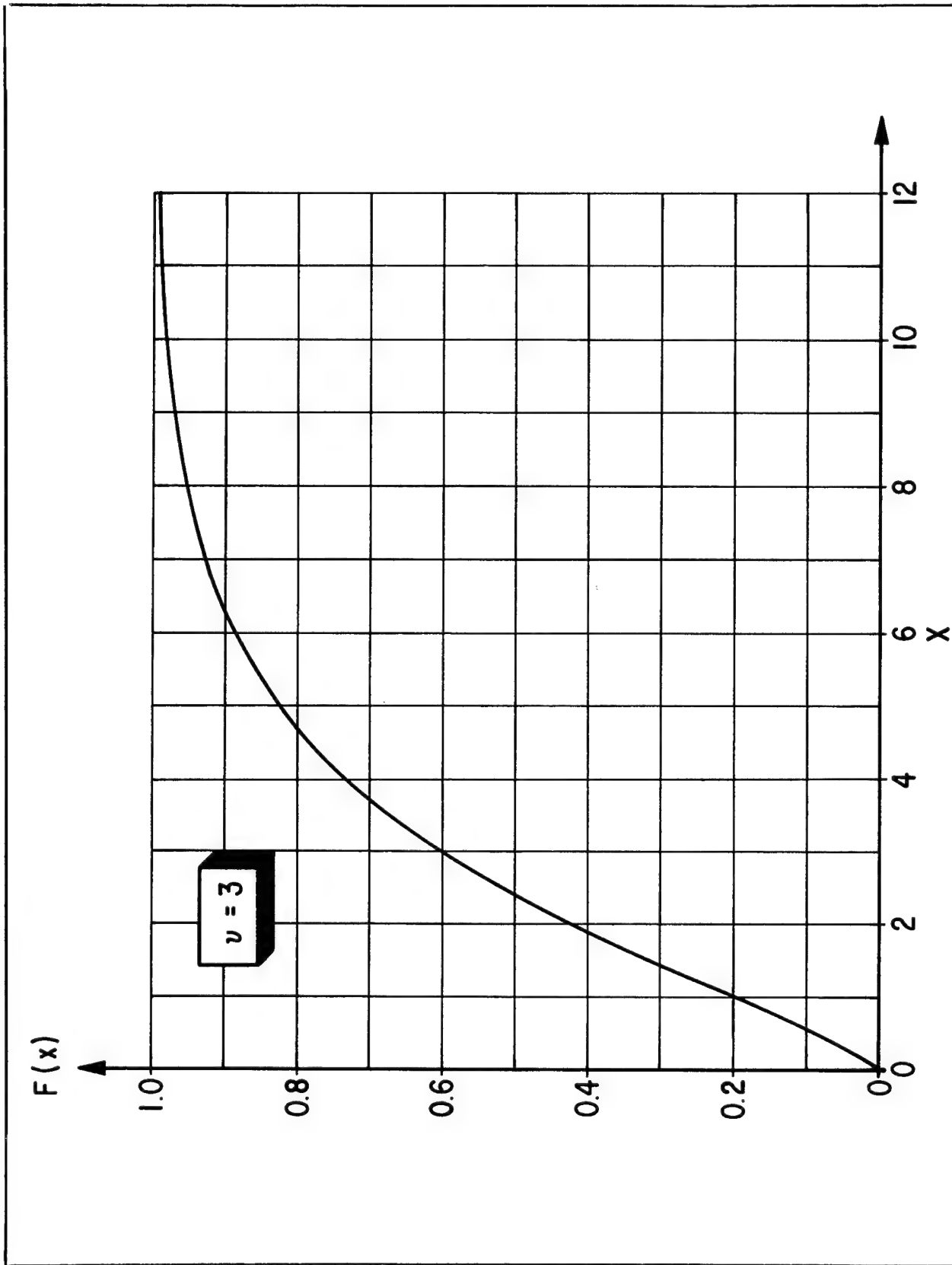


FIGURE 5. CHI-SQUARE DISTRIBUTION FUNCTION

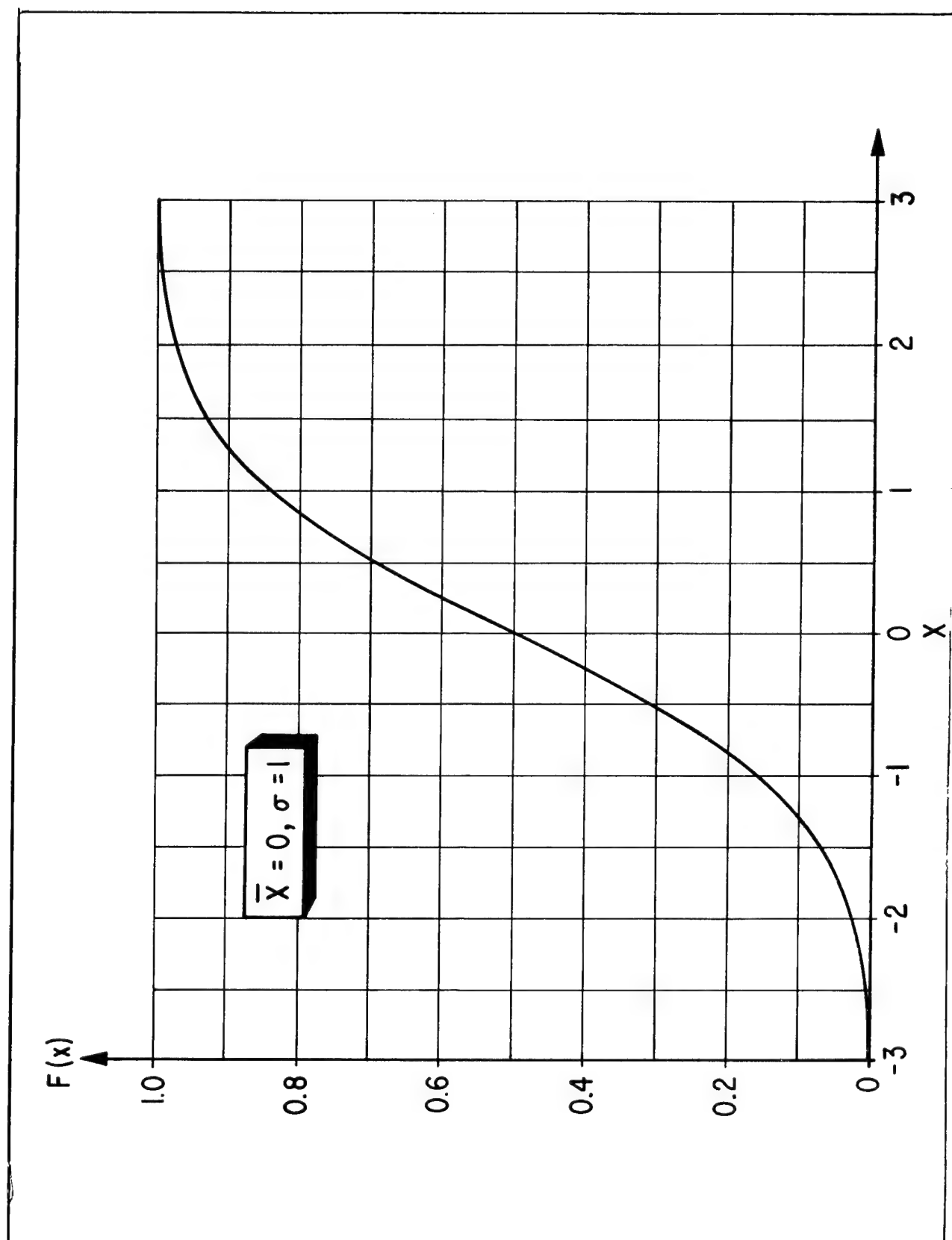


FIGURE 6. NORMAL DISTRIBUTION FUNCTION

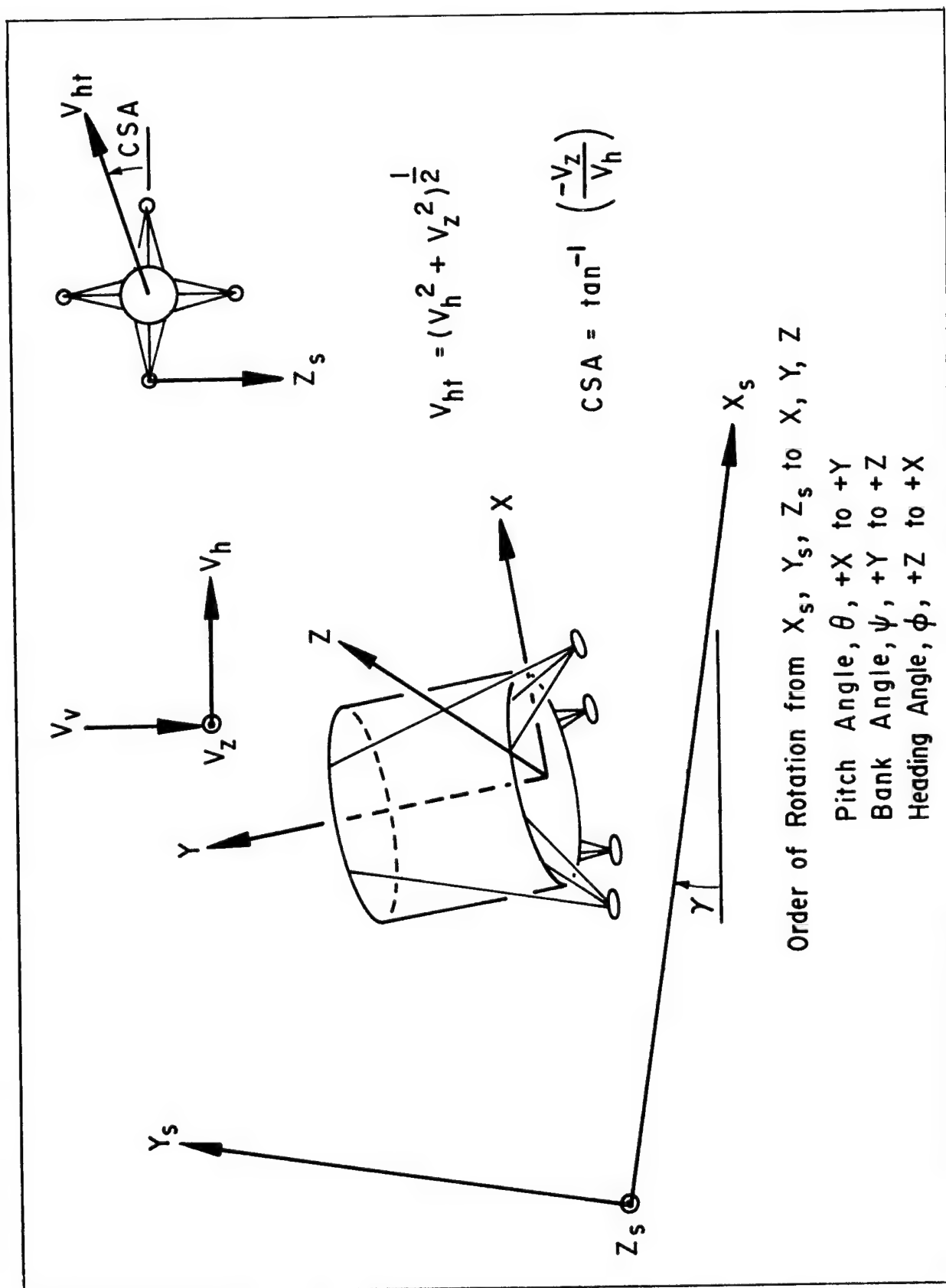


FIGURE 7. SURFACE AND BODY AXES ORIENTATION

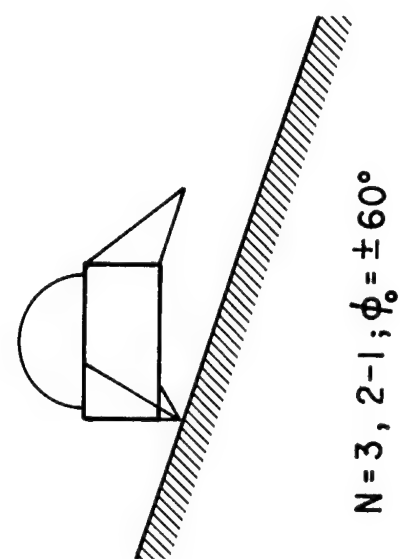
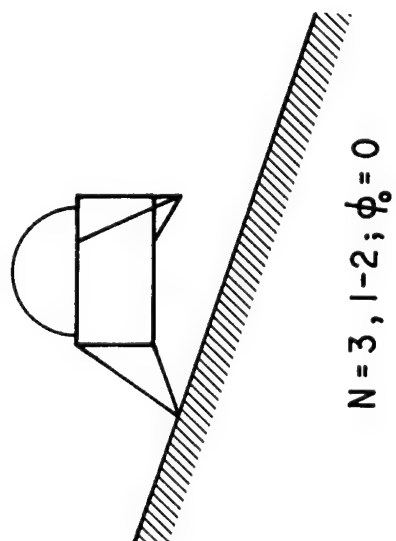
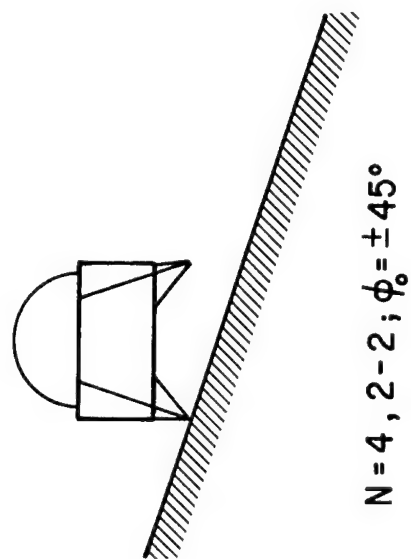
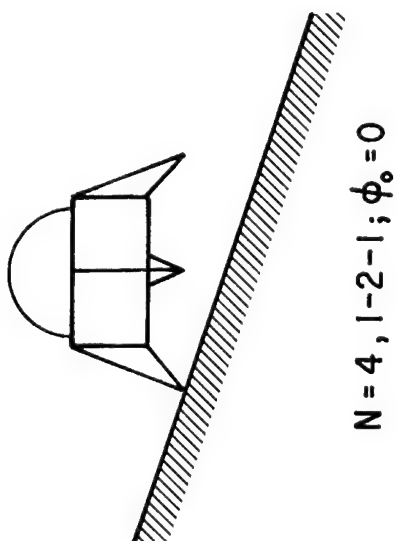


FIGURE 8. SYMMETRIC HEADING ORIENTATIONS

Lunar Slope, γ , deg

CSA = 30° , $V_v = 1.8$ m/sec, $V_{ht} = 0.9$ m/sec

$\theta_p = \psi_0 = \omega_x = \omega_y = \omega_z = 0$

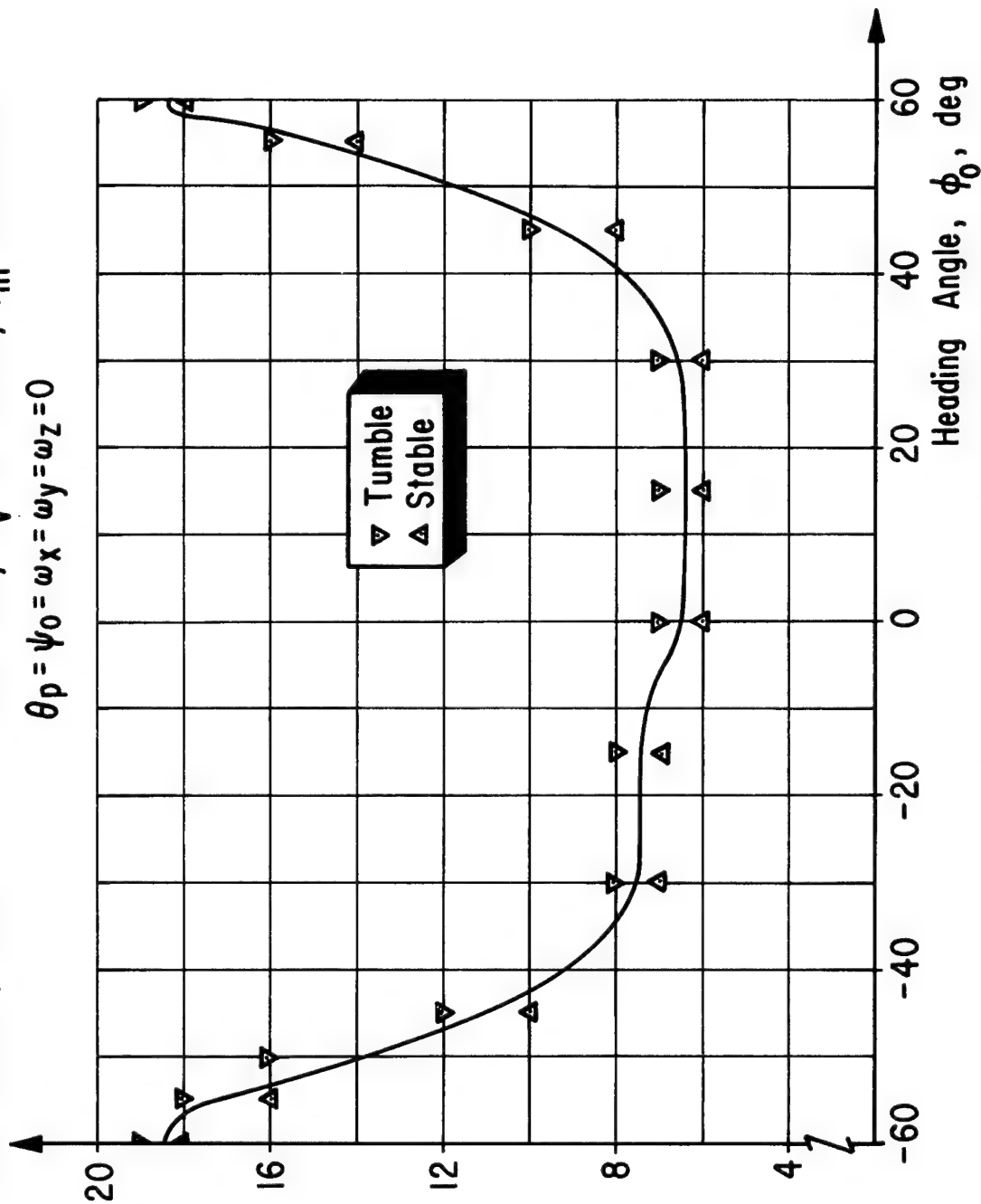


FIGURE 9. STABILITY BOUNDARY FOR VEHICLE 3

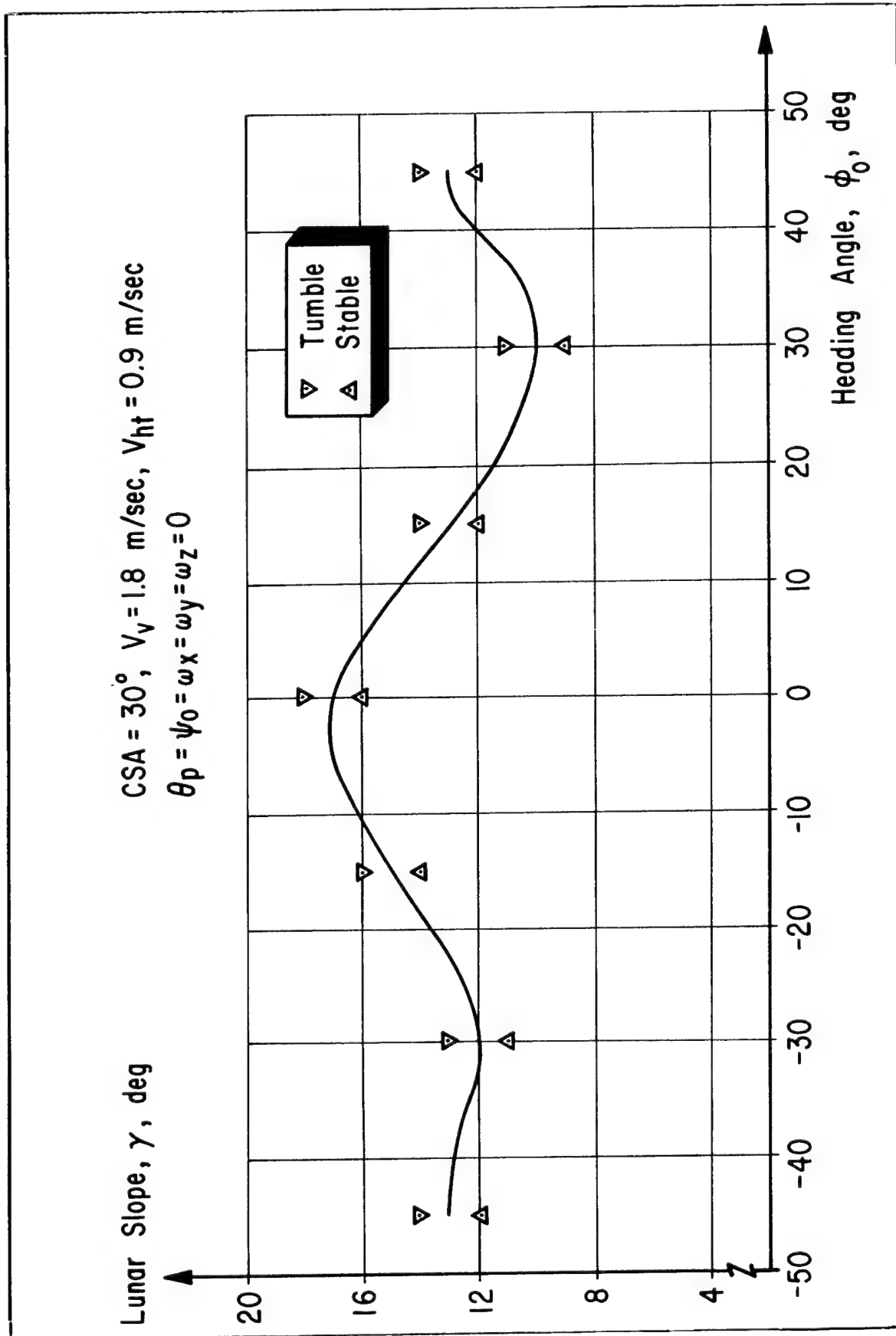


FIGURE 10. STABILITY BOUNDARY FOR VEHICLE 7

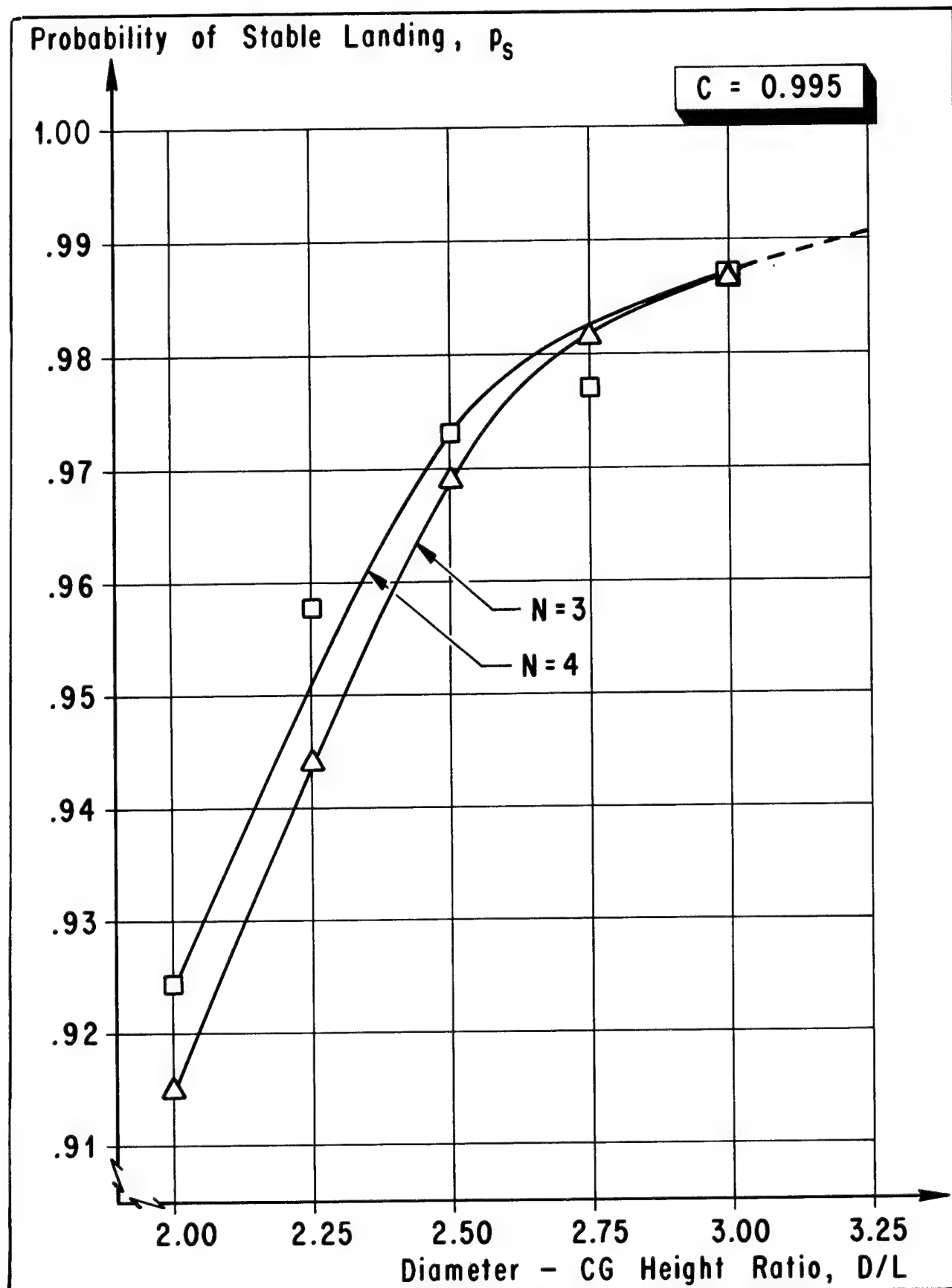


FIGURE 11. LOWER LIMIT PROBABILITY OF STABLE LANDING

TABLE 1. GEOMETRIC PROPERTIES OF LFV, LEM, AND LLS

Vehicle	D	L	Y_a	Y_p	r	k_z
	cm (in)	cm (in)	cm (in)	cm (in)	cm (in)	cm (in)
LFV	279 (110)	112 (44)	74 (29)	30 (12)	56 (22)	58 (23)
LEM	813 (320)	320 (126)	170 (67)	119 (47)	208 (82)	165 (65)
LLS	1966 (774)	605 (238)	381 (150)	180 (71)	330 (130)	259 (102)

Vehicle	D/L	Y_a/L	Y_p/L	r /L	k_z/L
LFV	2.50	0.66	0.27	0.50	0.52
LEM	2.54	0.53	0.37	0.65	0.52
LLS	3.25	0.63	0.30	0.55	0.43

TABLE 2. GEOMETRIC PROPERTIES OF VEHICLES I, II, AND III

Vehicle	Type	Y_a/L	Y_p/L	r /L	k_z/L
I	LFV	0.61	0.31	0.57	0.48
II	LEM	0.61	0.31	0.57	0.48
III	LLS	0.61	0.31	0.57	0.48

Vehicle	Type	Y_a	Y_p	r	k_z
		cm (in)	cm (in)	cm (in)	cm (in)
I	LFV	68 (27)	35 (14)	64 (25)	54 (21)
II	LEM	195 (77)	99 (39)	182 (72)	153 (60)
III	LLS	369 (145)	188 (74)	345 (136)	290 (114)

TABLE 3. LIMITING FORCES FOR TYPE I VEHICLES

Vehicle	N	D/L	C_{mp}		C_{sp}		k_v	
			N	lb	N	lb	N/cm	lb/in
1	3	2.00	3576	804	1192	268	8756	5000
2	3	2.25	3897	876	1299	292	7425	4240
3	3	2.50	4218	948	1406	316	6252	3570
4	3	3.00	4977	1119	1659	373	4588	2620
5	4	2.00	2682	603	894	201	8756	5000
6	4	2.25	2922	657	974	219	7425	4240
7	4	2.50	3162	711	1054	237	6252	3570
8	4	3.00	3738	840	1246	280	4588	2620

TABLE 4. DYNAMIC SCALING FACTORS

Quantity	Scale Factor	Vehicle Type	
		II	III
Acceleration	$g/g_I = \alpha$	1.00	1.00
Mass	$m/m_I = \beta$	14.00	42.00
Length	$L/L_I = \gamma$	2.86	5.41
Angular Acceleration	α/γ	0.35	0.18
Time	$(\gamma/\alpha)^{1/2}$	1.69	2.33
Angular Velocity	$(\alpha/\gamma)^{1/2}$	0.59	0.43
Angle	$(\alpha/\gamma)^0$	1.00	1.00
Velocity	$(\alpha \cdot \gamma)^{1/2}$	1.69	2.33
Force	$\alpha \cdot \beta$	14.00	42.00
Mass Density	β/γ^3	0.60	0.27
Moment of Inertia	$\beta \cdot \gamma^2$	115	1229
Stress	$\alpha \cdot \beta/\gamma^2$	1.71	1.44
Spring Rate	$\alpha \cdot \beta/\gamma$	4.90	7.76

TABLE 5. INITIAL CONDITIONS FROM CHI-SQUARE DISTRIBUTION

F (x)	%	20.000	50.000	80.000	90.000	95.000	99.000	99.865	99.997
X	-	1.005	2.366	4.642	6.251	7.815	11.341	16.022	21.000
\bar{V}_{ht}	-	0.061	0.143	0.281	0.378	0.473	0.686	0.970	1.271
\bar{V}_v	-	0.122	0.286	0.562	0.756	0.946	1.372	1.939	2.541
γ	deg	2.1	5.0*	9.8	13.2	16.5	24.0	33.9	44.4
$V_{ht, I}$	m/s	0.057	0.133	0.261	0.353	0.441	0.637	0.901	1.181
$V_{ht, II}$	m/s	0.096	0.224	0.442	0.594	0.744	1.078	1.524*	1.996
$V_{ht, III}$	m/s	0.133	0.310	0.608	0.819	1.024	1.486	2.100	2.752
V_v, I	m/s	0.114	0.266	0.522	0.706	0.882	1.274	1.802	2.362
V_v, II	m/s	0.192	0.448	0.884	1.188	1.488	2.156	3.048*	3.992
V_v, III	m/s	0.266	0.620	1.216	1.638	2.048	2.972	4.200	5.504

*Values used to establish multiplication constants.

TABLE 6. TABULATION OF DISTRIBUTION FUNCTIONS

Normal Distribution ($\bar{x} = 0, \sigma = 1$)		Chi-Square Distribution ($\nu = 3$)	
F(X)	X	F (X)	X
0.00000	-5.00	0	0
0.00003	-4.00	0.08111	0.50
0.00024	-3.50	0.19875	1.00
0.00135	-3.00	0.31773	1.50
0.00621	-2.50	0.42759	2.00
0.02275	-2.00	0.52444	2.50
0.04006	-1.75	0.60837	3.00
0.06681	-1.50	0.67900	3.50
0.10565	-1.25	0.73854	4.00
0.15866	-1.00	0.82820	5.00
0.22663	-0.75	0.88839	6.00
0.30854	-0.50	0.92810	7.00
0.40129	-0.25	0.95399	8.00
0.50000	0	0.97071	9.00
0.59871	0.25	0.98143	10.00
0.69146	0.50	0.99262	12.00
0.77337	0.75	0.99818	15.00
0.84134	1.00	0.99956	18.00
0.89435	1.25	0.99997	21.00
0.93319	1.50	1.00000	24.00
0.95994	1.75		
0.97725	2.00		
0.99379	2.50		
0.99865	3.00		
0.99976	3.50		
0.99997	4.00		
1.00000	5.00		

TABLE 7. SUMMARY OF TOUCHDOWN DYNAMICS RUNS FOR VEHICLE 1

Group A			Group B			Group C		
<u>Case</u>	<u>Result</u>	<u>γ, deg.</u>	<u>Case</u>	<u>Result</u>	<u>γ, deg.</u>	<u>Case</u>	<u>Result</u>	<u>γ, deg.</u>
6	S	13.0	145	S	10.4	13	S	14.8
8	S	10.3	168	S	12.7	61	S	9.5
9	S	11.8	172	S	1.7	95	S	8.4
14	S	14.2	235	S	10.0	100	S	14.3
39	S	15.7	238	S	9.7	102	S	13.9
43	T	6.9	242	S	12.4	103	S	4.9
46	S	8.9	247	S	8.4	123	S	8.0
64	S	12.4	250	S	8.0	243	S	12.2
66	S	12.8	259	S	6.8	337	S	8.3
82	S	15.3	275	S	13.4			
84	T	15.5	277	S	15.0			
87	T	11.5	288	S	12.4			
118	T	10.7	289	S	8.8			
120	S	10.3	291	S	7.2			
144	S	14.1	296	S	8.6			
148	S	11.8	303	S	9.5			
157	T	23.0	307	S	14.8			
158	S	16.0	309	S	10.7			
173	T	15.5	314	S	13.0			
177	T	19.3	315	S	12.1			
179	S	10.4	319	S	7.3			
187	S	9.1	321	S	13.5			
198	S	14.9	327	T	14.9			
206	S	16.8	338	S	6.9			
207	S	16.9	341	S	8.4			
211	S	11.3	357	S	15.3			
212	T	9.7	363	T	14.0			
214	S	11.3	364	S	15.4			

TABLE 7 (CONTINUED)

Group A			Group B		
<u>Case</u>	<u>Result</u>	<u>γ, deg.</u>	<u>Case</u>	<u>Result</u>	<u>γ, deg.</u>
215	S	17.7	368	S	14.1
234	S	14.4	369	T	12.5
294	S	16.4	386	S	9.5
299	S	11.6	396	S	13.3
328	S	17.7	397	S	8.7
332	S	19.2	400	S	6.7
333	S	16.3			
339	T	17.0			
345	S	17.2			
346	T	21.8	Group A: Cases which were thought to have a substantial probability of tumbling.		
350	T	20.6			
351	T	16.5	Group B: Cases which were believed, with substantial uncertainty, would be stable.		
371	T	21.2			
379	S	14.7	Group C: Cases which were thought, with only a small degree of uncertainty, would be stable.		
389	S	10.9			
390	S	18.3			
398	T	23.5			

TABLE 8. SUMMARY OF TOUCHDOWN DYNAMICS RUNS FOR VEHICLE 5

Group A			Group B			Group C		
Case	Result	γ , deg.	Case	Result	γ , deg.	Case	Result	γ , deg.
14	S	14.2	6	S	13.0	13	S	14.8
39	S	15.7	9	S	11.8	64	S	12.4
66	S	12.8	43	S	6.9	87	S	11.5
84	S	15.5	46	S	8.9	100	S	14.3
157	T	23.0	61	S	9.5	102	S	13.9
173	T	15.5	82	S	15.3	118	S	10.7
177	S	19.3	95	S	8.4	145	S	10.4
198	S	14.9	103	S	4.9	148	S	11.8
206	T	16.8	123	S	8.0	275	S	13.4
215	S	17.7	144	S	14.1	303	S	9.5
289	S	8.8	158	S	16.0	321	S	13.5
296	S	8.6	207	T	16.9	338	S	6.9
315	S	12.1	212	S	9.7	389	S	10.9
319	S	7.3	228	S	9.3	396	S	13.3
328	T	17.7	234	S	14.4			
333	S	16.3	238	S	9.7			
339	T	17.0	270	S	6.7			
346	T	21.8	277	S	15.0			
350	T	20.6	288	S	12.4			
351	T	16.5	291	S	7.2			
364	S	15.4	294	T	16.4			
368	S	14.1	307	S	14.8			
371	T	21.2	314	S	13.0	Group A: Cases which were thought to have a substantial probability of tumbling		
390	T	18.3	327	S	14.9			
398	T	23.5	332	T	19.2			
			337	S	8.3	Group B: Cases which were believed, with substantial uncertainty, would be stable		
			345	S	17.2			
			357	S	15.3			
			363	S	14.0	Group C: Cases which were thought, with only a small degree of uncertainty, would be stable		
			369	S	12.5			
			376	S	5.4			
			379	S	14.7			

TABLE 9. SUMMARY OF CASES WHICH TUMBLE

Case	Vehicle							
	1	2	3	4	5	6	7	8
36	T	T	T		T	T		
43	T							
84	T	T						
87	T							
118	T							
129	T	T			T	T	T	
157	T	T	T		T	T		
173	T	T			T			
177	T							
206					T			
207					T			
212	T							
294					T			
317	T	T	T		T	T	T	
327	T							
328					T			
332					T			
339	T	T			T			
346	T	T			T			
350	T	T			T	T		
351	T				T			
363	T							
369	T							
371	T	T	T		T	T		
390					T			
398	T	T			T	T	T	
n _f	20	11	4	0	17	7	3	0

TABLE 10. SAMPLE PROBABILITY OF STABLE LANDING

$\bar{p}_s = (400 - n_f) / 400$								
Vehicle	1	2	3	4	5	6	7	8
\bar{p}_s	0.9500	0.9725	0.9900	1.0000	0.9575	0.9825	0.9925	1.0000

TABLE 11. LOWER LIMIT PROBABILITY OF STABLE LANDING

<u>C = 0.950</u>								
Vehicle	1	2	3	4	5	6	7	8
p_s (Ref 23)	0.9282	0.9549	0.9773	0.9925	0.9369	0.9674	0.9807	0.9925
p_s (Ref 24)	0.9303	0.9575	0.9787	0.9925	0.9394	0.9696	0.9817	0.9925
<u>C = 0.995</u>								
Vehicle	1	2	3	4	5	6	7	8
p_s (Ref 23)	0.9149	0.9439	0.9689	0.9868	0.9243	0.9577	0.9728	0.9868
p_s (Ref 24)	0.9223	0.9498	0.9713	0.9868	0.9314	0.9620	0.9744	0.9868

APPENDIX A

TOUCHDOWN CONDITIONS

CASE NO.	WV	BAR	VH	CSA	PHIO	VV	VH	V7	THETA	GAMMA	PSI	PHI 3	PHI 4	WX	WY	W7	VHT
	IN/SEC	IN/SEC	DEG	DEG	DEG	IN/SEC	IN/SEC	IN/SEC	DEG	DEG	DEG	DEG	DEG	DEG/S	DEG/S	DEG/S	IN/SEC
56	0.917	0.331	25.0	309.1	33.6	11.0	-5.1	-1.3	3.9	0.7	-50.9	39.1	0.9	0.7	-4.2	12.1	12.1
57	0.857	0.354	34.4	85.4	31.4	1.3	-12.9	-0.9	1.1	3.9	-34.6	-4.6	-2.8	-1.1	1.9	12.9	12.9
58	0.575	0.084	133.7	1.7	21.1	-0.7	-3.0	1.4	1.0	1.7	1.7	1.7	0.4	-0.3	-1.1	3.1	3.1
59	0.336	0.031	42.9	57.9	12.3	0.1	-1.2	0.5	7.1	-0.9	57.9	-32.1	2.9	5.2	2.5	1.2	1.2
60	0.134	0.081	22.0	254.0	4.9	2.8	12.0	-0.3	9.5	-1.5	-39.9	-3.2	-3.8	-2.7	-0.4	3.0	3.0
61	0.521	0.331	281.1	230.1	19.1	-2.3	-7.1	-0.3	4.2	-4.3	-14.0	-3.8	2.7	0.6	11.0	11.0	11.0
62	0.120	0.301	140.0	346.0	4.4	-8.4	-7.1	-0.3	4.2	-4.3	-14.0	-3.8	2.7	0.6	11.0	11.0	11.0
63	0.297	0.054	318.9	241.9	10.9	1.5	1.3	1.8	4.6	1.0	1.9	-28.1	4.1	3.6	0.8	2.0	2.0
64	0.458	0.419	97.7	277.7	17.1	-2.1	-15.2	0.5	12.4	1.3	37.7	7.7	1.2	-1.0	0.2	15.3	15.3
65	0.594	0.022	196.5	93.4	21.7	-0.8	0.2	1.4	7.6	1.1	-26.6	3.4	-1.4	-2.3	-1.1	0.8	0.8
66	0.574	0.171	255.1	49.1	21.0	-1.6	6.0	-0.9	12.8	-3.4	49.1	-40.9	2.5	-0.4	-5.0	6.3	6.3
67	0.423	0.141	213.7	144.7	15.5	0.3	5.1	-1.3	4.8	-1.2	24.7	-35.3	-2.0	-4.3	0.8	5.1	5.1
68	0.251	0.275	252.2	20.2	9.2	-3.1	9.6	0.5	4.5	0.5	20.2	20.2	0.2	-4.1	-3.6	10.1	10.1
69	0.056	0.134	190.6	35.6	2.4	-4.9	0.9	-1.3	10.4	-0.5	35.6	35.6	1.5	-0.2	-0.3	5.0	5.0
70	0.384	0.161	89.0	190.9	14.0	0.1	-5.9	-1.4	5.9	-1.1	-49.1	10.9	2.1	-1.8	1.5	5.9	5.9
71	0.046	0.006	307.3	126.2	1.7	0.1	-0.2	2.8	8.0	-2.8	6.2	36.2	1.8	-0.5	2.7	0.2	0.2
72	0.215	0.344	125.5	201.4	7.9	-7.3	-0.2	1.8	2.5	1.4	-38.6	21.4	0.7	6.6	3.1	12.6	12.6
73	0.346	0.034	263.6	56.5	12.7	-0.2	1.4	-2.8	1.8	-1.0	56.5	-33.5	-1.2	4.3	2.2	1.4	1.4
74	0.423	0.244	1.6	51.5	15.5	9.9	-0.2	1.3	4.7	1.5	51.5	-38.5	4.8	-1.5	0.6	8.9	8.9
75	0.409	0.257	59.6	186.4	15.0	4.8	-8.1	1.7	1.9	-2.5	-53.6	6.4	-0.1	-5.9	-1.5	9.4	9.4
76	0.309	0.053	77.4	101.3	11.3	0.4	-1.9	-1.4	2.6	-0.9	-18.7	11.3	3.2	-3.0	3.1	1.9	1.9
77	0.170	0.528	55.2	156.1	6.2	11.0	-15.9	-2.9	8.3	-0.3	36.1	-23.9	-2.5	1.0	-1.1	19.3	19.3
78	0.921	0.048	353.0	350.8	33.7	1.8	0.2	-1.1	4.2	-0.2	-9.2	-9.2	-1.0	0.3	1.4	1.8	1.8
79	0.276	0.235	250.4	325.5	10.1	-2.9	8.1	2.5	11.2	-0.8	-34.5	-34.5	-0.5	2.5	4.5	8.6	8.6
80	0.787	0.217	138.2	80.0	28.8	-2.5	-7.5	-2.5	4.9	-2.3	-40.0	-10.0	-0.7	-0.0	-1.7	7.9	7.9
81	0.134	0.015	245.7	334.5	4.9	0.1	0.5	-1.2	5.2	1.7	-25.5	-25.5	1.9	0.4	-1.2	0.5	0.5
82	0.242	0.271	63.1	8.9	8.9	4.5	-8.8	-3.3	15.3	-0.7	8.9	8.9	5.4	-6.3	-5.1	9.9	9.9
83	0.300	0.394	160.4	183.2	11.0	-13.6	-4.8	-1.6	8.5	1.7	-56.8	3.2	0.7	2.8	2.6	14.4	14.4
84	0.288	0.121	217.7	137.5	10.6	-3.5	2.7	1.4	15.5	-2.1	17.5	-42.5	-3.2	-3.8	0.2	4.4	4.4
85	0.211	0.095	234.8	231.6	7.7	-2.0	2.8	1.1	5.2	-0.7	-8.4	-38.4	0.1	1.4	-1.4	3.5	3.5
86	0.094	0.180	211.9	105.7	3.1	-5.9	3.7	-3.8	4.9	-0.1	-14.3	15.7	2.4	1.4	0.5	6.9	6.9
87	0.537	0.087	148.9	119.7	19.6	-2.8	-1.7	1.3	11.5	-0.1	-0.3	29.7	6.7	-3.5	4.1	3.3	3.3
88	0.179	0.100	45.9	273.7	6.6	2.8	-2.9	2.1	6.3	-0.6	33.7	3.7	-4.2	3.2	-2.5	4.0	4.0
89	0.494	0.314	262.8	207.5	17.7	-1.5	1.5	-0.8	8.5	-2.0	-32.5	27.5	-5.7	-4.4	-1.3	11.6	11.6
90	0.039	0.219	79.5	281.5	1.4	1.5	-1.9	-1.5	2.7	1.9	41.3	11.3	3.0	0.8	-1.1	8.0	8.0
91	0.149	0.430	216.2	135.0	5.5	-12.7	9.3	0.0	2.0	-0.6	15.0	-45.0	0.7	0.4	-1.8	15.7	15.7
92	0.194	0.163	312.9	128.6	7.2	4.1	4.4	-2.0	4.9	1.9	8.6	38.6	-2.0	3.5	-4.3	6.0	6.0
93	0.185	0.160	9.4	262.2	6.8	6.1	-1.0	-1.6	2.0	-2.0	22.2	-7.8	1.7	0.9	1.8	6.2	6.2
94	0.117	0.582	25.9	175.6	4.3	10.2	-9.3	0.8	2.7	-0.6	55.6	-4.4	-2.9	1.8	-1.2	21.3	21.3
95	0.942	0.263	2.3	229.0	34.5	9.6	-0.4	-0.1	8.4	-0.0	-11.0	-41.0	-0.5	-1.9	2.2	9.6	9.6
96	0.352	0.470	298.6	62.3	12.9	8.4	15.4	1.0	6.2	0.0	-57.7	-27.7	0.7	-3.0	-2.8	17.5	17.5
97	0.085	0.150	194.8	35.6	3.1	-5.3	1.4	-1.1	11.1	-0.6	35.6	35.6	1.2	-0.6	-0.7	5.5	5.5
98	0.321	0.134	51.0	148.7	11.8	3.2	-3.9	-1.2	4.8	-1.9	28.7	-31.3	0.9	-3.7	0.2	5.0	5.0
99	0.673	0.303	227.1	41.8	24.6	-7.5	8.1	-0.8	5.1	2.0	41.8	41.8	-0.2	-2.9	0.3	11.1	11.1
100	0.044	0.164	3.1	74.8	1.7	6.1	-0.3	-0.3	14.3	-0.6	-45.2	-15.2	-2.2	0.6	-0.3	6.1	6.1
101	0.094	0.217	99.0	247.7	3.5	-1.2	-7.8	0.5	8.1	2.0	7.7	-22.3	2.6	-0.5	-1.7	7.9	7.9
102	0.085	0.062	154.9	200.5	3.1	-2.0	-1.0	-2.2	13.9	-0.9	-39.5	23.5	-1.1	1.1	1.1	4.5	4.5
103	1.531	0.034	170.6	293.3	56.8	-1.3	-0.2	-2.9	4.9	-0.6	53.3	23.3	1.8	-1.7	0.2	1.3	1.3
104	0.498	0.112	146.3	166.0	18.2	-3.4	-2.3	-0.5	4.6	-0.0	46.0	-14.0	-5.2	-1.7	4.6	4.1	4.1
105	0.223	0.024	81.9	178.6	8.1	0.1	-1.0	-2.5	10.3	-0.0	58.6	-1.4	-2.2	1.1	-1.1	1.0	1.0
106	0.836	0.044	337.5	331.1	30.6	1.6	0.6	-1.5	5.8	-0.6	-28.9	-28.9	-1.7	-0.4	0.6	1.7	1.7
107	0.197	0.179	192.9	263.6	7.2	-6.4	1.5	1.1	7.7	-2.0	23.6	-6.4	-2.0	0.7	1.6	6.5	6.5
108	0.403	0.127	8.3	335.9	14.7	4.6	-0.7	0.4	2.3	1.9	-24.1	-24.1	-4.1	-2.7	1.8	4.6	4.6
109	0.654	0.215	143.6	188.2	23.9	-6.3	-4.6	2.1	1.5	-0.6	-51.8	8.2	2.3	-3.4	1.1	7.8	7.8
110	0.900	0.087	238.8	180.5	32.9	-1.6	2.7	0.0	4.3	1.9	-59.5	0.5	-0.6	-0.4	-0.4	3.2	3.2

CASE	NO.	VV	BAR	VH	CSA	PHIO	VV	VH	VZ	THETA	GAMMA	PSI	PHI 3	PHI 4	WX	WY	WZ	VHT
		IN/SEC	DEG	IN/SEC	DEG	IN/SEC	IN/SEC	IN/SEC	IN/SEC	DEG	DEG	DEG	DEG	DEG	DEG/S	DEG/S	DEG/S	IN/SEC
111	0.807	0.090	294.0	312.6	29.5	1.3	3.0	0.2	1.4	-2.0	-47.4	42.6	3.9	-2.6	-1.0	3.3	3.3	3.3
112	0.539	0.230	309.0	224.6	19.7	5.3	6.5	4.3	2.1	-0.6	-15.4	44.6	-1.2	-1.6	0.8	2.0	-2.5	8.4
113	0.308	0.145	284.0	276.6	11.3	1.3	5.1	1.7	7.2	-0.1	-36.6	6.6	2.1	1.1	0.2	7.8	5.3	8.4
114	0.108	0.213	218.9	108.5	3.9	-6.1	4.9	-4.5	5.3	-0.1	-11.5	18.5	2.1	1.1	0.2	7.8	5.3	8.4
115	0.448	0.073	113.8	80.4	16.4	-1.1	-2.4	0.6	9.1	-0.7	-39.6	-9.6	2.8	4.2	2.0	2.7	3.4	2.3
116	0.092	0.062	328.5	192.1	3.0	1.9	1.2	0.5	4.0	-2.2	-47.9	12.1	2.3	0.7	3.4	3.7	3.4	2.3
117	0.243	0.150	143.2	83.8	8.9	-4.7	-3.5	4.1	4.2	1.7	-36.2	-6.2	1.0	1.1	3.7	5.8	5.8	5.8
118	0.378	0.081	277.8	115.4	13.8	0.4	2.9	1.3	10.7	-0.8	-46.8	25.4	-0.9	-3.4	2.5	3.0	3.0	3.0
119	0.456	0.113	12.3	286.9	16.7	4.1	-0.9	2.6	6.7	1.6	46.9	16.9	6.3	4.1	0.8	4.1	0.8	4.1
120	0.429	0.395	66.8	238.3	15.7	5.7	-13.3	-0.3	10.3	-2.3	-1.7	-31.7	3.3	-2.7	-1.4	14.5	14.5	14.5
121	0.318	0.289	81.1	329.7	11.6	1.6	-10.4	-0.7	3.9	-0.8	-30.3	-30.3	3.3	2.0	7.1	10.6	10.6	10.6
122	0.171	0.104	55.4	200.9	6.3	0.7	-1.0	1.0	3.6	-0.3	-39.1	20.9	-2.5	1.9	1.9	1.2	1.2	1.2
123	0.897	0.263	349.6	212.1	32.5	9.5	1.7	-0.5	4.0	-0.3	-27.9	32.1	-1.1	-2.8	1.3	9.6	9.6	9.6
124	0.265	0.309	243.7	3.3	9.7	-5.0	10.1	-0.0	4.5	-0.9	3.3	3.3	-1.0	-3.7	3.9	11.3	11.3	11.3
125	0.712	0.083	97.8	294.3	26.1	-0.4	-3.0	4.5	4.0	-2.6	54.3	24.3	-1.0	-3.7	3.9	3.0	3.0	3.0
126	0.115	0.043	271.8	5.3	4.2	0.0	1.6	2.2	1.3	1.4	5.3	5.3	-2.3	1.0	0.6	5.4	5.4	5.4
127	0.217	0.102	45.7	216.2	7.9	2.6	-2.7	-2.3	3.2	-1.0	-23.8	36.2	3.9	0.6	5.4	3.7	3.7	3.7
128	0.255	0.588	139.5	207.0	9.7	-16.4	-14.0	1.5	3.1	1.3	-33.0	27.0	0.3	3.7	2.0	21.5	21.5	21.5
129	0.247	0.654	193.2	337.7	9.0	-23.4	5.5	1.8	2.3	1.0	-22.3	-22.3	-4.6	0.9	-0.3	24.0	24.0	24.0
130	0.170	0.109	206.9	248.3	6.2	-3.5	1.8	-1.4	2.9	-1.1	8.3	-21.7	-0.4	1.7	-5.4	4.0	4.0	4.0
131	0.033	0.052	180.5	298.9	1.2	-1.9	0.0	3.0	5.4	-0.5	58.9	28.9	1.6	-2.0	-0.1	1.9	1.9	1.9
132	0.427	0.097	114.0	126.4	15.6	-1.4	-3.3	-1.2	3.8	-0.6	9.4	39.4	3.3	-3.2	-2.6	3.6	3.6	3.6
133	0.126	0.384	7.4	198.8	4.6	14.0	-1.8	2.2	6.6	-1.2	-20.2	9.8	4.5	-0.7	-4.0	14.1	14.1	14.1
134	0.376	0.329	220.7	210.2	13.8	-9.1	7.9	2.1	2.6	-3.5	-29.8	30.2	3.5	-4.3	-2.3	12.0	12.0	12.0
135	0.844	0.059	34.0	100.4	30.9	1.8	-1.2	-1.5	2.7	1.0	-19.6	10.4	1.7	-3.4	-2.2	2.2	2.2	2.2
136	0.090	0.415	167.2	130.6	2.9	-14.4	-3.4	4.5	7.3	-1.4	10.6	40.6	-0.3	0.3	-3.3	15.2	15.2	15.2
137	0.122	0.015	280.3	300.7	4.5	-0.1	0.5	-2.2	4.7	0.9	-59.3	30.7	-3.9	-0.9	3.6	0.5	0.5	0.5
138	0.106	0.159	313.3	250.7	3.9	4.0	4.2	0.9	7.0	-5.0	10.7	-19.3	0.5	0.6	0.6	5.8	5.8	5.8
139	0.021	0.125	326.3	340.7	0.8	3.8	2.5	0.5	2.3	-1.5	-19.3	-19.3	5.1	-2.3	-2.8	4.6	4.6	4.6
140	0.533	0.234	299.2	210.6	18.5	4.2	7.5	2.8	2.0	-0.9	-29.4	30.6	-1.8	-2.4	0.8	8.6	8.6	8.6
141	0.233	0.112	212.0	220.4	8.5	-2.5	3.2	0.6	5.4	-1.0	-19.6	40.4	-0.6	0.5	4.7	4.1	4.1	4.1
142	0.879	0.130	124.7	10.1	32.2	-2.7	-3.9	1.2	2.8	-1.7	10.1	10.1	-0.2	-1.1	-2.3	4.7	4.7	4.7
143	0.198	0.387	337.4	299.7	7.3	13.1	5.5	-1.7	4.0	3.6	59.7	29.7	-0.5	0.0	-1.3	14.2	14.2	14.2
144	0.398	0.244	149.9	9.3	14.6	-7.7	-4.5	-2.9	14.1	0.6	9.3	9.3	-1.8	-4.4	-1.2	8.9	8.9	8.9
145	0.628	0.534	282.4	218.8	23.0	4.2	19.1	-0.9	10.4	-2.0	-21.2	38.8	5.7	6.4	-2.0	19.6	19.6	19.6
146	0.818	0.172	14.8	208.2	30.0	6.1	-1.6	4.1	1.3	0.5	-31.8	28.2	0.6	-1.3	-5.5	6.3	6.3	6.3
147	0.722	0.174	67.1	337.5	26.4	2.5	-5.9	-4.4	9.8	2.9	-22.5	-22.5	-3.6	-5.1	1.4	6.4	6.4	6.4
148	0.490	0.594	79.4	246.7	17.9	4.0	-21.4	-0.3	11.8	-2.2	6.7	-23.3	-0.1	-3.0	-1.7	21.8	21.8	21.8
149	0.280	0.257	51.6	295.9	10.2	5.8	-7.4	-1.3	3.2	-1.5	55.9	25.9	1.9	0.9	1.6	9.4	9.4	9.4
150	0.081	0.429	343.7	125.0	3.0	15.1	4.4	-0.2	1.9	-1.5	5.0	35.0	4.0	0.0	-4.0	15.7	15.7	15.7
151	0.393	0.140	235.7	94.0	14.4	-2.9	4.2	-3.3	4.0	-2.6	-26.0	4.0	5.9	2.0	-1.4	5.1	5.1	5.1
152	0.041	0.124	87.6	202.9	1.5	0.2	-4.5	-3.8	0.4	2.2	-37.1	22.9	4.0	-0.5	-0.5	4.5	4.5	4.5
153	0.202	0.264	259.5	91.8	7.4	-1.8	9.5	-0.5	0.6	0.1	-28.2	1.8	1.9	-0.1	-0.5	9.7	9.7	9.7
154	0.316	0.142	31.3	120.6	11.6	4.5	-2.7	-2.0	4.4	-3.0	0.6	30.6	-0.1	3.7	-1.2	5.2	5.2	5.2
155	0.373	0.182	123.0	289.3	13.6	-3.6	-5.6	-1.0	2.5	-0.0	49.3	19.3	3.6	1.7	-3.2	6.7	6.7	6.7
156	0.346	0.039	174.6	237.9	12.7	-1.4	-0.1	2.0	4.1	1.8	-2.1	-32.1	0.6	4.5	2.3	1.4	1.4	1.4
157	0.250	0.001	186.2	326.4	9.1	-0.0	0.0	1.4	21.0	-3.8	-33.6	-33.6	5.5	0.4	-1.0	0.0	0.0	0.0
158	0.113	0.081	157.6	194.9	4.1	-2.8	-1.1	-2.9	15.0	-2.3	-45.1	14.9	-1.8	0.3	2.5	3.0	3.0	3.0
159	0.586	0.472	89.0	203.3	21.5	0.3	-17.3	1.5	2.9	-2.4	-36.7	23.3	-0.5	3.9	-2.7	17.3	17.3	17.3
160	0.191	0.002	340.4	351.6	7.0	0.1	0.0	2.2	0.3	4.9	-8.4	-8.4	-0.2	1.3	-0.8	0.1	0.1	0.1
161	0.491	0.128	191.6	279.8	18.0	-4.6	0.9	-0.8	1.6	1.4	39.8	9.8	-0.6	2.8	0.1	4.7	4.7	4.7
162	0.031	0.082	2.8	348.0	1.1	3.0	-0.1	-1.6	7.1	-0.5	-12.0	-12.0	-1.9	-0.7	0.1	3.0	3.0	3.0
163	0.136	0.144	133.8	196.0	5.0	-3.7	-3.8	-0.2	5.7	3.3	-44.0	16.0	5.0	-1.2	-0.6	5.3	5.3	5.3
164	0.174	0.040	224.8	184.0	6.4	-1.0	1.0	-2.4	11.2	-0.6	-56.0	4.0	0.5	1.0	-2.3	1.5	1.5	1.5
165	0.156	0.040	275.8	312.0	5.7	0.1	1.4	-2.1	5.3	1.1	-48.0	42.0	-4.0	-1.0	3.2	1.5	1.5	1.5

CASE	NO.	WV	BAR	WV	CSA	PHIO	WV	IN/SEC	VH	VZ	THETA	GAMMA	PSI	PHI 3	PHI 4	WX	WY	W7	VHT
						DEG		IN/SEC		IN/SEC	DEG		DEG	DEG	DEG	NEG/S	DEG/S	DEG/S	IN/SEC
166	0.030	0.146	286.6	219.8	2.9	1.5	5.1	0.3	6.1	0.6	0.6	0.6	5.2	27.6	-2.4	1.7	4.4	3.4	3.0
167	0.659	0.082	257.4	267.6	24.5	-0.7	2.9	0.7	0.4	12.7	0.4	12.7	4.8	-24.8	5.2	3.4	2.5	-2.0	4.7
168	0.281	0.128	188.1	95.2	10.3	0.0	-0.1	2.0	1.4	2.2	2.2	2.2	2.2	-27.2	-2.2	4.4	-3.7	-0.3	0.1
169	0.006	0.001	78.7	62.8	0.2	0.0	0.0	0.0	0.0	0.0	0.0	0.0	0.0	0.0	0.0	0.0	0.0	0.0	0.0
170	0.235	0.468	289.2	170.4	8.6	5.6	16.2	-2.2	8.5	0.7	5.8	0.7	5.8	32.2	-9.6	3.3	1.8	0.6	3.0
171	0.456	0.081	99.7	57.8	16.7	-0.5	-2.9	0.0	8.8	-1.2	5.7	1.8	-34.8	-4.8	-0.5	-2.1	-0.1	4.0	4.4
172	0.748	1.103	230.1	85.2	27.4	-25.9	31.0	-1.3	1.7	1.8	12.5	-1.4	12.5	-17.5	-4.8	-4.9	-1.7	1.4	1.4
173	1.074	0.037	320.4	252.5	39.3	1.1	0.9	-0.3	15.5	-1.4	3.0	0.3	4.3	19.7	0.2	-1.9	4.2	6.6	6.6
174	0.838	0.181	10.6	199.7	31.4	6.5	-1.2	3.0	1.3	0.3	0.3	0.3	0.3	0.3	0.3	0.3	0.3	0.3	0.3
175	0.541	0.142	20.7	286.8	19.8	4.8	-1.8	2.1	7.4	1.5	4.6	1.6	4.6	16.8	3.8	2.7	0.0	5.2	5.2
176	0.300	0.262	350.8	153.9	11.0	9.5	1.5	-2.0	6.7	2.2	33.9	-26.1	-2.4	2.6	3.4	2.6	4.5	9.6	9.6
177	0.095	0.123	280.8	160.9	3.5	0.8	4.4	3.2	19.3	2.1	40.9	-19.1	-1.0	-2.3	-1.5	4.5	4.5	4.5	4.5
178	0.411	0.139	170.7	307.8	15.0	-5.0	-0.8	3.2	7.8	1.2	-5.2	37.8	-0.7	5.0	0.1	5.1	5.1	5.1	5.1
179	0.052	0.421	20.5	234.6	1.9	14.4	-5.4	-0.4	10.4	-0.1	-5.4	-35.4	-1.1	-3.2	0.9	15.4	15.4	15.4	15.4
180	0.207	0.254	190.3	301.3	7.6	-9.1	1.7	-1.2	3.3	-2.3	-5.7	31.3	-2.6	1.1	1.0	9.3	9.3	9.3	9.3
181	0.318	0.568	320.0	148.0	11.6	15.9	13.4	0.2	2.3	0.9	28.0	-32.0	0.2	0.6	0.2	20.8	20.8	20.8	20.8
182	0.370	0.172	49.6	134.6	13.5	4.1	-4.8	-1.9	5.1	-2.6	14.6	44.6	-0.1	3.6	-1.3	6.3	6.3	6.3	6.3
183	0.340	0.171	99.1	261.1	12.4	-1.0	-6.2	-1.7	2.0	-0.5	21.1	-8.9	5.5	0.8	4.0	6.2	6.2	6.2	6.2
184	0.241	0.516	108.5	167.6	8.8	-6.0	-17.9	0.6	2.5	0.6	47.6	-12.4	-1.0	1.5	0.3	18.9	18.9	18.9	18.9
185	0.102	0.241	77.9	213.9	3.7	1.9	-8.6	-0.4	7.7	1.1	-20.1	33.9	0.9	-2.3	4.6	8.8	8.8	8.8	8.8
186	0.551	0.578	7.2	40.2	20.2	13.7	-1.7	0.6	5.4	1.0	40.2	40.2	2.2	-4.0	-1.2	13.8	13.8	13.8	13.8
187	0.174	0.128	256.4	6.4	6.4	-1.1	4.5	-1.7	9.1	0.3	6.4	6.4	2.7	-1.2	0.4	4.7	4.7	4.7	4.7
188	0.451	0.110	105.5	112.5	16.5	-1.1	-3.9	-0.9	3.8	-1.0	-5.5	22.5	0.7	-5.8	1.2	4.0	4.0	4.0	4.0
189	1.778	0.231	274.5	558.5	65.1	0.7	8.4	0.2	3.8	3.6	-1.5	-1.5	0.7	-5.8	1.2	8.4	8.4	8.4	8.4
190	0.110	0.123	43.5	24.5	4.0	3.3	-3.1	-1.1	9.5	-0.0	24.5	24.5	-1.3	-0.4	0.4	4.5	4.5	4.5	4.5
191	0.146	0.154	132.4	190.4	5.3	-3.9	-4.2	-0.4	5.8	2.9	-49.6	10.4	3.7	-1.7	-1.1	5.7	5.7	5.7	5.7
192	0.124	0.012	131.2	136.2	4.5	-0.4	0.0	3.4	8.4	-1.4	16.2	-43.8	-0.6	-0.2	-4.3	0.4	0.4	0.4	0.4
193	0.039	0.403	190.0	221.9	1.4	-14.5	2.6	-2.3	3.0	-0.3	-18.1	41.9	2.2	-4.2	0.5	14.7	14.7	14.7	14.7
194	0.549	0.057	158.6	87.6	20.1	-1.9	-0.8	-1.9	2.5	0.2	-32.4	-2.4	-4.4	-4.4	-4.4	-4.4	-4.4	-4.4	-4.4
195	0.233	0.320	87.2	93.2	8.5	0.6	-1.7	2.3	6.0	0.0	-26.8	3.2	-2.2	-0.6	-0.6	-0.6	-0.6	-0.6	-0.6
196	0.833	0.373	335.7	238.7	30.5	12.4	5.6	3.3	3.1	-0.6	-1.3	-31.3	-1.8	-2.6	0.5	13.6	13.6	13.6	13.6
197	0.195	0.095	184.1	164.1	6.8	-3.5	0.3	-0.4	4.2	-2.2	44.1	-15.9	-2.4	-1.3	1.3	3.5	3.5	3.5	3.5
198	0.368	0.050	352.5	229.4	13.5	1.8	0.2	-1.2	14.9	1.5	-10.6	-40.6	-6.0	2.9	1.3	1.8	1.8	1.8	1.8
199	0.558	0.104	120.8	74.7	20.4	-2.0	-3.3	0.1	10.4	-1.0	-45.3	-15.3	1.6	2.1	0.5	3.9	3.9	3.9	3.9
200	0.670	0.575	208.9	59.9	24.5	-4.4	19.1	-2.0	1.3	1.3	59.9	-30.1	-1.2	-3.5	-1.0	21.0	21.0	21.0	21.0
201	0.589	0.535	257.1	185.0	21.6	-4.4	19.1	-1.8	9.3	-3.4	-55.0	5.0	2.5	2.3	-5.6	19.6	19.6	19.6	19.6
202	0.408	0.090	245.1	90.0	14.9	-0.3	3.6	0.5	10.7	-1.4	-30.0	-0.0	-2.3	3.4	0.5	3.6	3.6	3.6	3.6
203	0.224	0.040	233.1	134.9	8.2	-0.9	1.2	-0.5	2.8	-0.9	14.9	44.9	-0.3	-0.9	-5.6	1.5	1.5	1.5	1.5
204	0.012	0.081	160.9	319.8	0.4	-2.8	-1.0	0.5	1.4	-1.0	-40.2	-40.2	0.8	-1.9	-0.0	2.9	2.9	2.9	2.9
205	0.304	0.299	48.7	284.6	11.1	7.2	-8.2	-1.9	3.4	-1.8	44.6	14.6	1.1	0.0	0.5	10.9	10.9	10.9	10.9
206	0.840	0.255	256.5	294.3	30.8	-0.3	9.1	-2.1	14.8	3.0	29.3	29.3	0.6	-2.9	1.3	9.3	9.3	9.3	9.3
207	0.129	0.031	44.1	274.0	4.7	0.5	-1.0	0.0	14.9	0.4	34.0	4.0	-0.6	-2.5	1.3	1.1	1.1	1.1	1.1
208	0.222	0.280	191.7	298.5	8.1	-10.0	2.1	-1.4	3.4	-2.5	58.5	28.5	-3.2	0.7	0.5	10.3	10.3	10.3	10.3
209	0.250	0.376	279.2	103.0	9.5	2.2	1.6	-0.6	1.4	0.2	-17.0	13.0	1.6	-0.6	-1.1	13.7	13.7	13.7	13.7
210	0.232	0.110	326.6	47.4	8.5	3.4	2.2	2.7	2.9	2.0	47.4	-42.6	-2.2	0.8	-6.2	4.0	4.0	4.0	4.0
211	0.148	0.077	333.9	131.7	5.4	2.5	1.2	1.8	11.3	-3.6	11.7	41.7	0.6	-2.2	0.5	2.8	2.8	2.8	2.8
212	1.038	0.154	301.2	356.0	46.0	2.9	4.8	-2.4	9.7	-2.3	-4.0	-4.0	-0.6	-2.4	-6.6	5.6	5.6	5.6	5.6
213	0.350	0.058	228.3	0.1	13.2	-1.4	1.6	1.8	1.5	-2.6	0.1	0.1	-7.9	0.4	-1.1	2.1	2.1	2.1	2.1
214	0.077	0.060	115.4	144.2	2.8	-1.1	-2.3	2.4	11.3	3.6	24.2	-35.8	-4.6	-1.3	0.4	2.5	2.5	2.5	2.5
215	0.233	0.207	322.4	68.2	10.7	6.0	4.6	-0.8	17.7	1.2	-51.8	-21.8	5.3	-0.3	1.2	7.6	7.6	7.6	7.6
216	0.561	0.141	129.4	132.2	20.5	-3.3	-4.0	-1.6	4.6	-0.7	12.2	42.2	2.2	6.2	1.2	5.1	5.1	5.1	5.1
217	1.036	0.223	256.2	336.0	39.7	-1.9	7.9	-0.2	3.5	2.4	-24.0	-24.0	0.0	3.6	0.3	8.1	8.1	8.1	8.1
218	0.035	0.084	343.0	0.9	0.9	3.0	0.9	-0.8	4.6	-1.0	-40.2	-40.2	-3.5	-2.1	-4.2	3.2	3.2	3.2	3.2
219	1.300	0.083	29.7	83.5	47.6	2.6	-1.5	-2.5	2.9	0.6	-36.5	-6.5	0.6	3.8	6.2	3.0	3.0	3.0	3.0
220	0.602	0.204	36.4	347.1	22.0	6.1	-4.5	0.1	3.4	1.8	-12.9	-12.9	4.7	-6.8	0.3	7.5	7.5	7.5	7.5

43

CASE	NO.	WV	BAR	VH	CSA	PHIO	WV	VH	VZ	THETA	GAMMA	PSI	PHT. 3	PHT. 4	WV	WV	WV	VHT
										DEG	DEG	DEG	DEG	DEG	DEG/S	DEG/S	DEG/S	IN/SEC
331		0.084	0.136	46.5	83.4	3.1	3.4	-3.6	-6.6	3.8	3.8	0.3	-36.6	-6.6	1.7	1.9	5.0	
332		0.236	0.109	244.4	178.3	10.5	-1.7	3.6	3.4	19.2	-1.1	58.3	-1.7	-1.1	-1.1	2.6	4.0	
333		0.211	0.212	42.2	53.1	18.7	5.8	-5.2	-1.1	16.3	2.7	53.1	-36.9	-2.9	-1.0	2.4	7.8	
334		0.755	0.104	160.0	67.9	28.7	3.6	-1.3	-5.6	3.1	0.4	-52.2	22.2	2.5	1.9	1.2	3.8	
335		0.930	0.125	275.6	222.5	34.0	-2.4	3.9	-2.5	0.8	1.8	-17.5	42.5	-0.7	0.3	-0.6	4.6	
336		0.574	0.384	275.2	157.0	25.4	1.3	14.0	0.5	2.1	-2.7	37.0	-23.0	2.9	1.5	4.4	14.1	
337		0.832	0.252	272.7	231.5	15.8	0.4	9.2	-0.0	2.3	0.9	-38.1	-4.1	-0.4	-2.0	7.0	27.9	
338		0.222	0.763	230.1	85.9	8.1	-17.9	21.4	1.4	6.9	-0.9	-38.1	-4.1	-0.4	-2.0	7.0	27.9	
339		1.271	0.188	147.4	80.2	46.5	-5.8	-3.7	-0.4	17.0	-1.2	-39.8	-9.8	0.6	0.4	-1.4	6.9	
340		0.256	0.195	24.6	214.5	9.7	6.5	-3.0	-0.1	7.0	-2.5	-35.5	34.5	0.6	-1.5	-1.1	7.1	
341		0.020	0.017	221.8	128.6	22.7	-0.5	0.4	2.8	8.4	1.9	8.6	38.6	-0.1	-0.6	0.5	0.6	
342		0.057	0.315	18.9	182.7	2.5	10.9	-3.7	1.3	2.2	-0.3	-87.3	2.7	-1.6	3.8	0.3	1.5	
343		0.143	0.009	135.9	16.7	5.2	-0.2	-0.2	3.5	1.9	3.3	16.7	16.7	2.4	-0.7	0.3		
344		0.151	0.177	212.9	350.7	5.9	-5.4	3.5	0.3	3.2	-0.8	-9.3	-9.3	0.2	-3.6	-2.9	6.5	
345		0.123	0.163	249.7	104.5	4.5	-2.1	5.6	0.3	17.2	0.6	-15.5	14.5	5.9	2.0	2.1	6.0	
346		0.012	0.391	246.5	358.3	0.4	-5.7	13.1	3.2	21.8	1.6	-1.7	-1.7	-1.2	2.5	-1.4	14.3	
347		0.453	0.197	203.2	32.0	16.9	-4.6	2.8	1.1	4.0	2.1	32.0	32.0	0.4	-1.6	1.6	7.2	
348		0.177	0.264	119.9	205.6	6.5	-4.8	-8.4	2.3	2.2	1.6	-34.4	25.6	1.3	-3.3	-5.6	9.7	
349		0.550	0.083	356.4	159.2	20.1	3.0	0.2	-0.4	3.9	0.7	39.2	-20.8	1.4	-1.1	-2.2	3.0	
350		0.099	0.059	192.9	252.6	3.6	-2.1	0.5	-0.7	20.6	-0.8	12.6	-17.4	0.7	4.6	-1.5	2.1	
351		0.234	0.139	349.3	126.0	8.5	5.0	0.9	1.0	14.5	3.6	6.0	36.0	-0.7	4.7	-1.8	5.1	
352		0.326	0.052	105.6	139.3	11.9	-0.5	-1.8	-0.5	3.1	-0.2	19.3	-40.7	-4.0	-1.0	-3.3	1.9	
353		0.351	0.070	181.8	292.6	12.8	-2.6	0.1	0.0	0.7	2.1	52.6	22.6	1.0	-3.0	2.9	2.6	
354		0.596	0.220	218.0	225.7	10.8	-6.3	4.9	5.6	2.1	-2.2	-14.3	-44.3	-3.6	-1.4	-0.1	8.0	
355		0.196	0.158	214.1	298.8	6.8	-4.8	3.2	2.3	4.1	-1.1	58.8	28.8	-0.4	2.9	-6.1	5.8	
356		0.019	0.269	170.1	151.8	0.7	-9.7	-1.7	-2.1	6.7	-0.8	31.8	-28.2	1.2	2.4	-0.5	9.8	
357		0.318	0.114	86.0	144.7	13.5	4.2	3.4	2.7	15.3	-1.1	24.7	-35.3	2.2	-2.9	1.6	4.2	
358		0.056	0.118	321.9	277.5	2.4	3.4	2.7	2.1	6.6	-2.3	37.5	7.5	2.3	3.0	3.7	4.3	
359		0.261	0.296	157.6	190.3	9.6	-10.0	-4.1	-1.1	7.9	2.1	-9.7	10.3	1.5	5.7	4.5	10.8	
360		0.458	0.182	313.3	243.0	16.8	4.6	4.8	-2.5	1.9	0.6	-3.0	-27.0	-0.1	-0.1	4.6	6.7	
361		0.651	0.276	58.9	75.6	24.2	3.6	-9.4	-0.9	0.4	3.2	-44.4	-14.4	-2.6	-0.9	2.4	10.1	
362		0.726	0.102	144.5	48.1	26.6	-3.0	-2.2	2.9	2.8	-0.8	48.1	-41.9	1.7	1.1	0.4	3.7	
363		0.579	0.090	179.9	160.6	21.2	3.3	-0.0	2.8	14.0	0.6	40.6	-19.4	-2.4	-1.3	-2.4	3.3	
364		0.372	0.204	175.3	52.9	13.6	-7.4	-0.6	-1.1	15.4	1.6	52.9	-37.1	0.2	-0.9	1.5	7.5	
365		0.181	0.112	130.6	85.2	6.6	-2.7	3.1	-3.1	3.5	2.0	-34.8	-4.8	1.9	2.5	-3.3	4.1	
366		0.771	0.149	45.8	257.4	28.2	3.8	-3.9	-1.6	1.7	1.6	17.4	-12.6	3.2	1.1	-0.6	5.5	
367		0.215	0.011	241.0	209.6	7.9	0.1	0.4	1.4	3.4	0.6	-30.4	28.6	3.3	3.2	0.7	0.4	
368		0.490	0.424	116.0	301.6	17.9	-6.8	-14.0	1.0	14.1	-0.8	-58.4	31.6	2.2	-0.1	1.2	15.6	
369		1.650	0.065	271.0	173.6	50.4	0.0	2.4	-4.3	12.5	3.2	53.6	-6.4	0.5	-0.1	1.0	2.4	
370		0.089	0.374	25.9	185.5	3.3	12.3	-6.0	1.2	2.5	-0.3	-54.5	5.5	-1.8	3.2	-0.1	13.7	
371		0.105	0.512	100.8	337.3	3.8	-3.5	-18.4	1.9	21.2	1.9	-22.7	-22.7	2.4	1.1	-2.0	18.7	
372		0.053	0.118	135.5	269.1	2.3	-3.1	-3.0	-1.0	1.4	-2.5	29.1	-0.9	-1.7	2.5	2.9	4.3	
373		0.742	0.074	130.2	340.8	27.1	-1.8	-2.1	-1.7	6.7	-1.5	-19.2	-19.2	0.7	-0.9	-0.8	2.8	
374		0.350	0.141	84.8	192.4	12.8	0.5	-5.2	-0.2	5.5	-1.0	-47.6	12.4	2.6	-1.3	2.2	5.2	
375		0.109	0.039	359.3	183.9	4.0	1.4	0.0	-2.4	11.1	-1.3	-56.1	3.9	4.5	1.0	-3.8	1.4	
376		0.397	0.041	233.8	315.3	14.5	-0.9	1.2	-2.0	5.4	-2.8	-44.7	-44.7	4.7	-0.9	-1.7	1.5	
377		0.008	0.151	68.1	226.7	0.3	2.1	-5.1	0.4	4.3	1.7	-13.3	-43.3	2.9	-0.1	-1.1	5.5	
378		0.153	0.084	222.4	277.9	5.6	-2.4	2.2	-0.5	0.9	-0.5	37.9	7.9	1.0	5.4	-1.4	3.2	
379		0.227	0.139	336.6	109.1	8.3	4.7	2.0	0.6	14.7	2.6	-10.9	19.1	-1.3	3.0	-2.8	5.1	
380		0.243	0.018	50.7	80.2	8.9	0.4	-0.5	-1.6	1.8	-1.1	-39.8	-9.8	3.1	-2.9	3.3	0.7	
381		0.197	0.001	84.8	191.3	7.2	0.0	-0.0	-1.7	0.9	0.3	-48.7	11.3	-1.3	2.3	0.1	0.0	
382		0.096	0.098	78.8	82.3	3.5	0.7	-3.5	0.4	10.3	1.2	-37.7	-7.7	-1.1	2.9	-4.9	3.6	
383		0.639	0.027	32.7	113.1	23.4	0.8	-0.5	-0.8	2.4	1.5	-6.9	23.1	3.3	-1.4	-0.4	1.0	
384		0.242	0.059	306.5	284.0	8.9	1.3	1.7	-0.0	0.3	1.1	44.0	14.0	-7.3	-3.1	1.7	2.2	
385		0.750	0.222	130.2	234.7	27.8	-8.1	0.0	-3.8	2.2	0.2	-5.3	-35.3	-6.5	-1.1	3.8	8.1	

CASE NO.	VV BAR	VH BAR	CSA DEG	PHIO DEG	VW IN/SEC	VH IN/SEC	VZ IN/SEC	THETA DEG	GAMMA DEG	PSI DEG	PHI 3 DEG	PHI 4 DEG	WX DEG/S	WY DEG/S	WZ DEG/S	VHT IN/SEC
386	0.152	0.177	13.9	325.3	5.6	6.3	-1.6	3.5	9.5	-1.3	-34.7	-34.7	3.5	4.6	6.3	6.5
387	0.293	0.356	157.5	185.9	10.7	-12.7	-2.8	-1.2	8.6	2.1	-44.1	15.9	1.3	4.5	4.4	13.0
388	0.395	0.162	241.0	206.4	14.5	1.1	5.8	4.9	1.2	-0.8	-33.6	26.4	-1.0	-1.2	2.3	5.9
389	0.418	0.185	354.4	356.8	15.3	6.8	0.7	-2.8	10.9	1.2	-3.2	-3.2	-3.7	-3.4	0.2	6.8
390	0.348	0.024	27.7	287.2	12.7	0.8	-0.4	0.3	18.3	-5.8	47.2	17.2	-1.0	-1.7	-2.7	0.9
391	0.222	0.393	21.0	357.4	8.1	13.4	-5.2	-0.3	4.8	-2.0	-2.6	-2.6	1.4	2.5	1.2	14.4
392	0.052	0.044	334.2	207.6	2.3	1.5	0.7	1.1	3.9	-1.6	-32.4	27.6	3.9	1.9	-3.9	1.6
393	0.411	0.252	247.3	197.7	15.0	-3.4	8.5	-0.8	7.5	-2.1	-42.3	17.7	-4.8	-3.7	-0.9	9.2
394	0.038	0.256	120.3	327.7	3.2	-4.7	-8.1	-0.6	3.6	3.8	-32.3	-32.3	-4.7	2.3	0.3	9.4
395	0.282	0.040	313.3	237.7	10.3	1.2	1.3	1.9	4.4	1.0	-2.3	-32.3	4.1	3.6	0.8	1.8
396	0.434	0.444	106.2	287.6	17.7	-4.5	-15.6	0.7	13.3	-1.1	47.6	17.6	1.5	-0.7	0.5	16.2
397	0.698	0.037	219.0	117.4	25.6	-1.1	0.9	2.0	8.7	1.5	-2.6	27.4	-0.8	-1.5	-0.5	1.4
398	0.758	0.207	291.7	87.1	27.7	2.8	7.1	-0.3	23.5	-2.0	-32.9	-2.9	4.2	0.4	-2.7	7.6
399	0.587	0.186	324.3	196.7	21.3	5.5	4.0	-0.4	4.4	-0.4	-43.3	16.7	-0.8	-2.1	2.1	6.8
400	0.357	0.490	316.9	86.3	13.4	13.1	12.3	1.6	4.7	0.4	-33.7	-3.7	1.6	-1.7	-1.5	17.9

APPENDIX B
RANDOM NUMBER GENERATOR CONFIDENCE TEST

RANDOM NUMBER GENERATOR CONFIDENCE TEST FOR A FLAT DISTRIBUTION.

FOR RNI 1)	OBS.FREQ	EXP.FREQ	O-E	(O-E)**2	(O-E)**2/E
PARTITION [1]	44	40	4	16.0	0.40
PARTITION [2]	38	40	-2	4.0	0.10
PARTITION [3]	39	40	-1	1.0	0.02
PARTITION [4]	40	40	0	0.	0.
PARTITION [5]	45	40	5	25.0	0.62
PARTITION [6]	45	40	5	25.0	0.62
PARTITION [7]	43	40	3	9.0	0.22
PARTITION [8]	40	40	0	0.	0.
PARTITION [9]	38	40	-2	4.0	0.10
PARTITION [10]	28	40	-12	144.0	3.60

CHI SQUARED 5.70 VARIANCE 0.07873 MEAN 0.484644

FOR RNI 2)	OBS.FREQ	EXP.FREQ	O-E	(O-E)**2	(O-E)**2/E
PARTITION [1]	34	40	-6	36.0	0.90
PARTITION [2]	45	40	5	25.0	0.62
PARTITION [3]	46	40	6	36.0	0.90
PARTITION [4]	36	40	-4	16.0	0.40
PARTITION [5]	33	40	-7	49.0	1.22
PARTITION [6]	39	40	-1	1.0	0.02
PARTITION [7]	49	40	9	81.0	2.02
PARTITION [8]	37	40	-3	9.0	0.22
PARTITION [9]	37	40	-3	9.0	0.22
PARTITION [10]	44	40	4	16.0	0.40

CHI SQUARED 6.95 VARIANCE 0.08475 MEAN 0.506417

RANDOM NUMBER GENERATOR CONFIDENCE TEST FOR A FLAT DISTRIBUTION.

FOR RNI 3)	OBS.FREQ	EXP.FREQ	O-E	(O-E)**2	(O-E)**2/E
PARTITION [1]	32	40	-8	64.0	1.60
PARTITION [2]	40	40	0	0.	0.
PARTITION [3]	35	40	-5	25.0	0.62
PARTITION [4]	46	40	6	36.0	0.90
PARTITION [5]	36	40	-4	16.0	0.40
PARTITION [6]	49	40	9	81.0	2.02
PARTITION [7]	41	40	1	1.0	0.02
PARTITION [8]	38	40	-2	4.0	0.10
PARTITION [9]	38	40	-2	4.0	0.10
PARTITION [10]	45	40	5	25.0	0.62

CHI SQUARED 5.40 VARIANCE 0.08038 MEAN 0.512077

FOR RNI 4)	OBS.FREQ	EXP.FREQ	O-E	(O-E)**2	(O-E)**2/E
PARTITION [1]	34	40	-6	36.0	0.90
PARTITION [2]	35	40	-5	25.0	0.62
PARTITION [3]	44	40	4	16.0	0.40
PARTITION [4]	33	40	-7	49.0	1.22
PARTITION [5]	38	40	-2	4.0	0.10
PARTITION [6]	49	40	9	81.0	2.02
PARTITION [7]	39	40	-1	1.0	0.02
PARTITION [8]	42	40	2	4.0	0.10
PARTITION [9]	49	40	9	81.0	2.02
PARTITION [10]	37	40	-3	9.0	0.22

CHI SQUARED 7.65 VARIANCE 0.08002 MEAN 0.519123

RANDOM NUMBER GENERATOR CONFIDENCE TEST FOR A FLAT DISTRIBUTION.

FOR RN[5]	OBS.FREQ	EXP.FREQ	O-E	(O-E)**2	(O-E)**2/E
PARTITION [1]	39	40	-1	1.0	0.02
PARTITION [2]	56	40	16	256.0	6.40
PARTITION [3]	43	40	3	9.0	0.22
PARTITION [4]	41	40	1	1.0	0.02
PARTITION [5]	36	40	-4	16.0	0.40
PARTITION [6]	38	40	-2	4.0	0.10
PARTITION [7]	29	40	-11	121.0	3.03
PARTITION [8]	38	40	-2	4.0	0.10
PARTITION [9]	45	40	5	25.0	0.62
PARTITION [10]	35	40	-5	25.0	0.62

CHI SQUARED 11.55 VARIANCE 0.08562 MEAN 0.477556

FOR RN[6]	OBS.FREQ	EXP.FREQ	O-E	(O-E)**2	(O-E)**2/E
PARTITION [1]	38	40	-2	4.0	0.10
PARTITION [2]	44	40	4	16.0	0.40
PARTITION [3]	37	40	-3	9.0	0.22
PARTITION [4]	47	40	7	49.0	1.22
PARTITION [5]	43	40	3	9.0	0.22
PARTITION [6]	32	40	-8	64.0	1.60
PARTITION [7]	45	40	5	25.0	0.62
PARTITION [8]	31	40	-9	81.0	2.02
PARTITION [9]	43	40	3	9.0	0.22
PARTITION [10]	40	40	0	0.	0.

CHI SQUARED 6.65 VARIANCE 0.06253 MEAN 0.494876

RANDOM NUMBER GENERATOR CONFIDENCE TEST FOR A FLAT DISTRIBUTION.

FOR RNI 7)	OBS.FREQ	EXP.FREQ	O-E	(O-E)**2	(O-E)**2/E
PARTITION (1)	41	40	1	1.0	0.02
PARTITION (2)	45	40	5	25.0	0.62
PARTITION (3)	36	40	-4	16.0	0.40
PARTITION (4)	35	40	-5	25.0	0.62
PARTITION (5)	44	40	4	16.0	0.40
PARTITION (6)	43	40	3	9.0	0.22
PARTITION (7)	36	40	-4	16.0	0.40
PARTITION (8)	41	40	1	1.0	0.02
PARTITION (9)	39	40	-1	1.0	0.02
PARTITION (10)	40	40	0	0.	0.

CHI SQUARED 2.75 VARIANCE 0.08516 MEAN 0.498583

FOR RNI 8)	OBS.FREQ	EXP.FREQ	O-E	(O-E)**2	(O-E)**2/E
PARTITION (1)	50	40	10	100.0	2.50
PARTITION (2)	38	40	-2	4.0	0.10
PARTITION (3)	30	40	-10	100.0	2.50
PARTITION (4)	35	40	-5	25.0	0.62
PARTITION (5)	45	40	5	25.0	0.62
PARTITION (6)	36	40	-4	16.0	0.40
PARTITION (7)	35	40	-5	25.0	0.62
PARTITION (8)	50	40	10	100.0	2.50
PARTITION (9)	34	40	-6	36.0	0.90
PARTITION (10)	47	40	7	49.0	1.22

CHI SQUARED 12.00 VARIANCE 0.09170 MEAN 0.506176

RANDOM NUMBER GENERATOR CONFIDENCE TEST FOR A FLAT DISTRIBUTION.

FOR RN[9]	OBS.FREQ	EXP.FREQ	O-E	(O-E)**2	(O-E)**2/E
PARTITION [1]	45	40	5	25.0	0.62
PARTITION [2]	34	40	-6	36.0	0.90
PARTITION [3]	39	40	-1	1.0	0.02
PARTITION [4]	35	40	-5	25.0	0.62
PARTITION [5]	41	40	1	1.0	0.02
PARTITION [6]	33	40	-7	49.0	1.22
PARTITION [7]	41	40	1	1.0	0.02
PARTITION [8]	43	40	3	9.0	0.22
PARTITION [9]	50	40	10	100.0	2.50
PARTITION [10]	39	40	-1	1.0	0.02

CHI SQUARED 6.20 VARIANCE 0.08505 MEAN 0.510156

FOR RN[10]	OBS.FREQ	EXP.FREQ	O-E	(O-E)**2	(O-E)**2/E
PARTITION [1]	46	40	6	36.0	0.90
PARTITION [2]	32	40	-8	64.0	1.60
PARTITION [3]	36	40	-4	16.0	0.40
PARTITION [4]	44	40	4	16.0	0.40
PARTITION [5]	39	40	-1	1.0	0.02
PARTITION [6]	48	40	8	64.0	1.60
PARTITION [7]	49	40	9	81.0	2.02
PARTITION [8]	35	40	-5	25.0	0.62
PARTITION [9]	36	40	-4	16.0	0.40
PARTITION [10]	35	40	-5	25.0	0.62

CHI SQUARED 8.60 VARIANCE 0.08003 MEAN 0.495523

"The aeronautical and space activities of the United States shall be conducted so as to contribute . . . to the expansion of human knowledge of phenomena in the atmosphere and space. The Administration shall provide for the widest practicable and appropriate dissemination of information concerning its activities and the results thereof."

—NATIONAL AERONAUTICS AND SPACE ACT OF 1958

NASA SCIENTIFIC AND TECHNICAL PUBLICATIONS

TECHNICAL REPORTS: Scientific and technical information considered important, complete, and a lasting contribution to existing knowledge.

TECHNICAL NOTES: Information less broad in scope but nevertheless of importance as a contribution to existing knowledge.

TECHNICAL MEMORANDUMS: Information receiving limited distribution because of preliminary data, security classification, or other reasons.

CONTRACTOR REPORTS: Technical information generated in connection with a NASA contract or grant and released under NASA auspices.

TECHNICAL TRANSLATIONS: Information published in a foreign language considered to merit NASA distribution in English.

TECHNICAL REPRINTS: Information derived from NASA activities and initially published in the form of journal articles.

SPECIAL PUBLICATIONS: Information derived from or of value to NASA activities but not necessarily reporting the results of individual NASA-programmed scientific efforts. Publications include conference proceedings, monographs, data compilations, handbooks, sourcebooks, and special bibliographies.

Details on the availability of these publications may be obtained from:

SCIENTIFIC AND TECHNICAL INFORMATION DIVISION
NATIONAL AERONAUTICS AND SPACE ADMINISTRATION
Washington, D.C. 20546